TRANSCRIPTION PROFILING OF ANGIOGENESIS USING DNA MICROARRAYS

by

Adam Budoff

A Thesis Submitted to the Faculty of the

GRADUATE INTERDISCIPLINARY PROGRAM IN
BIOMEDICAL ENGINEERING

In Partial Fulfillment of the Requirements
For the Degree of

MASTER OF SCIENCE
WITH A DEGREE IN BIOMEDICAL ENGINEERING

In the Graduate College

THE UNIVERSITY OF ARIZONA

2000

STATEMENT BY AUTHOR

This thesis has been submitted in partial fulfillment of requirements for an advanced degree at the University of Arizona and is deposited in the University Library to be made available to borrowers under the rules of the library.

Brief quotations from this thesis are allowable without special permission, provided that accurate acknowledgement of source is made. Requests for permission for extended quotation from or reproduction of this manuscript in whole or in part may be granted by the copyright holder.

SIGNED: _____

APPROVAL BY THESIS DIRECTOR

This thesis has been approved on the date shown below:

_____ _____

James B. Hoying
Assistant Professor of Biomedical Engineering

6/30/00
Date

ACKNOWLEDGEMENTS

I would like express my gratitude to my thesis advisor and mentor, Dr. Jay Hoying. Your guidance and scientific advice has and will continue to have a lasting impression on my all my future scientific endeavors. I am very grateful to have had the privilege and opportunity to work in your lab.

A sincere thank you to my committee members, Dr. Stuart Williams and Dr. David Galbraith. Your oversight on particular aspects of the project was invaluable to my graduate studies.

I would also like to thank the other members of the Hoying lab for providing a stimulating scientific environment with which to be a part of. It was a privilege to work with them. Additionally, I would like to extend my gratitude to the people in the Williams lab and the Galbraith lab for always being there to help and for providing expert advice.

TABLE OF CONTENTS

STATEMENT BY AUTHOR..... 2

ACKNOWLEDGEMENTS..... 3

LIST OF FIGURES..... 7

LIST OF TABLES..... 9

ABSTRACT..... 10

INTRODUCTION..... 11

cDNA Microarrays..... 11

Angiogenesis..... 18

MATERIALS AND METHODS..... 24

Arrayed Gene Sequences and Control Sequences..... 24

Primers..... 24

PCR Reactions and Components for the 58 Genes..... 26

PCR Reactions for the Control Genes..... 27

Electrophoresis of the PCR Products..... 27

PCR Product and Control Purification..... 29

Sequencing of Generated PCR Products..... 29

Coating of Slides..... 29

Printing of Arrayed Genes..... 31

Processing of Microarrays..... 35

II-4 Treatment of ePTFE..... 35

TABLE OF CONTENTS - *continued*

Polymer Implants..... 36

Mouse Tumors..... 37

Tumor/Polymer Explants and Tissue Preparation..... 37

Preparation of Labeled Probe..... 39

Purification of Labeled Probe..... 39

Hybridization of Microarrays..... 40

Scanning of Hybridized Microarrays..... 41

Analysis of Hybridized Microarrays..... 41

RESULTS..... 46

Microarray Elements are of Proper Size and Good Quality..... 46

Epoxide I is Comparable to the Commercial Slide Products..... 49

Quality Control Check of the PMT and Laser Settings for the Scanner..... 53

Verifying Printing of the 58-gene Big-Array..... 57

Il-4 vs. Unmodified Healing Tissue..... 66

Tumor vs. Normal Muscle Tissue..... 66

DISCUSSION..... 73

APPENDIX A

Primer Sequences..... 84

APPENDIX B

Protocols..... 87

TABLE OF CONTENTS - *continued*

REFERENCES..... 89

LIST OF FIGURES

FIGURE 1, Homologous Base Pairing Diagram..... 13

FIGURE 2, Scheme for Obtaining Differential Expression of RNA Transcripts..... 15

FIGURE 3, Non-Commercial Coating Chemistries..... 30

FIGURE 4, Prototype Microarray Layout..... 33

FIGURE 5, Big-Array Layout..... 34

FIGURE 6, Agarose Gel of Prototype Microarray Genes..... 47

FIGURE 7, Optimal Nucleotide Alignment Comparison Chart..... 48

FIGURE 8, Agarose Gel of PCR Products Amplified from Different Thermocycler Programs..... 50

FIGURE 9, Image of PCR Products Hybridized to Prototype Array 95..... 52

FIGURE 10, Fold Change Expression Pattern for Prototype Array 27..... 54

FIGURE 11, Raw Hybridization Intensities from Different Slide Chemistries..... 55

FIGURE 12, Raw Background Intensities from Different Slide Chemistries..... 56

FIGURE 13, Image of PCR Products Hybridized to Big-Array 16..... 59

FIGURE 14, Image of Labeled Mouse Heart cDNA with Cy-5 Hybridized to Big Array 12..... 61

LIST OF FIGURES – *continued*

FIGURE 15, Raw Cy-5 Hybridization Signals from 5 Genes on Big-Array 12 62

FIGURE 16, Mean Cy-5 Hybridization Signals of Triplicates from Big-Array 12 63

FIGURE 17, Image of Labeled Mouse Heart cDNA with Cy-3 and Cy-5 Hybridized to Big-Array 23 64

FIGURE 18, Scatter plot of Big-Array 23 65

FIGURE 19, Images of 5 Week Explant Tissue from Unmodified and II-4 Modified ePTFE 67

FIGURE 20, Image of II-4 Modified and Unmodified ePTFE Implant Tissue cDNA's Hybridized to Big-Array 5 68

FIGURE 21, Transcription Profile of Unmodified vs. II-4 Modified EPTFE Implant Tissue 69

FIGURE 22, Image of Tumor vs. Normal Mouse Thigh cDNA Hybridized to Big-Array 42 71

FIGURE 23, Transcription Profile of Tumor vs. Mouse Thigh Tissue 72

FIGURE 24, Gene Expression Differences in Different Angiogenic Phenotypes 80

FIGURE 25, Scatter plot of Different Angiogenic Phenotypes 81

LIST OF TABLES

TABLE I, List of All Genes Present on Prototype Arrays and Big-Arrays..... 25

TABLE II, Master PCR Program List..... 28

TABLE III, Mouse ePTFE Polymer Implant Chart..... 38

TABLE IV, Laser Settings Chart for Detectability of Signals from Prototype Arrays..... 58

ABSTRACT

Angiogenesis is the process by which new blood vessels form from an existing vasculature. The degree of angiogenesis and the character of the resulting microvascular beds vary between different healing environments such as wound healing and tumor angiogenesis. These differences are due, in part, to qualitative and quantitative differences in the molecular function within the tissue undergoing angiogenesis. For this study, these two types of angiogenic environments were created in mice and characterized on a gene expression level by utilizing cDNA microarrays. A DNA microarray containing 58 mouse genes from many different molecular classes relevant to angiogenesis was manufactured and tested. Optimal conditions and protocols for the use of microarray technology were designed and implemented. Results show that a polymer-induced angiogenic wound healing response differs greatly in its transcription profile from a tumor, suggesting that different types of angiogenesis occur in different environments.

INTRODUCTION

cDNA MICROARRAYS

With the advent of DNA sequencing and the recent surge in large scale DNA sequencing projects and comprehensive cDNA library surveys, the amount of sufficient data available regarding complete genomes has increased exponentially (13). Currently, the complete genomes of nearly a dozen microbes have been sequenced and in the next few years those of several more metazoans, including the entire human genome, are expected to be finished (10). With all or most of the sequence for many individual genes now available in data mines such as GenBank, gene expression studies from a global genome perspective are now possible. This transition from studying the interaction and function of one gene at a time to the interaction of thousands of genes simultaneously has spawned the new field of functional genomics (13).

Functional genomics attempts to assign function to genes based on when and where the mRNA corresponding to that gene is expressed in a given biological process. Function is also assigned based on gene homology and sequence domains. The developmental, histological, and physiological patterns in which a gene is expressed provide clues to its biological role since only a subset of all encoded genes are expressed in any given cell at given time (39) (27). With the advances in technology developed for the experimental use of the DNA sequence information generated, mRNA expression differences between different cell lines and tissue are now possible (48). One such technology used for this study is cDNA microarrays (49).

cDNA microarrays allow for the simultaneous expression monitoring of 1000's of mRNA's corresponding to genes in a particular cell state or condition (25) (50). This "chip-based" technology involves the immobilization of minute amounts of DNA sequences (often PCR products) on solid substrates, such as standard glass microscope slides. By using a printing robot (or arrayer), up to 50,000 different spots, each containing multiple copies of a particular DNA sequence, corresponding to a specific gene, can be printed onto a single microscope slide (12). The DNA sequences can be standard PCR products amplified by specific primer sets from known mRNA sequences or cDNA amplified from expression vectors containing a normalized cDNA library (thus containing known and unknown genes). The DNA sequences are attached to the slide using a variety of surface coatings, such as reactive aldehyde groups, poly-L-lysines, or epoxides. These surface coatings fasten the DNA sequences firmly to the surface of the slide through covalent or ionic bonding of the base pairs via a Schiff base reaction or an amide bond.

The basic premise behind DNA microarrays involves the fact that each DNA strand carries with it the capacity to recognize a uniquely complementary sequence through base pairing (Figure 1). This process of recognition, or hybridization, is extremely specific and highly parallel, thus allowing for the query of all spotted DNA sequences at the same time (7). Additionally, the sequence recognized can be of RNA, DNA, or cDNA origin. Therefore, DNA microarrays are basically an extension of classic Southern, Northern, and dot blots used to identify and quantify nucleic acid species in biological samples (43) (12). The amount of RNA (or DNA or cDNA) corresponding to

Figure 1.
Arrayed sections of genes on the glass slide hybridize with labeled cDNA probe from the two samples compared via complementary base pairing between homologous sections.

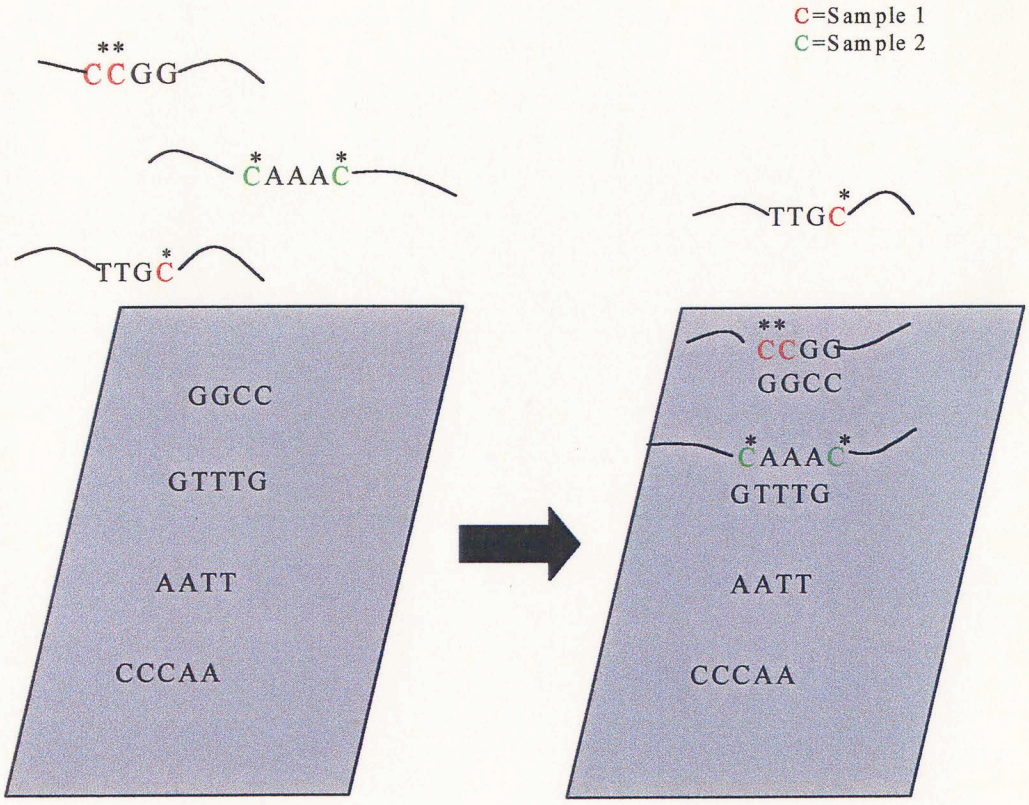

a gene that hybridizes to its complementary DNA sequence spotted on the microarray is indicative of its concentration (and thus expression level) in the particular RNA pool of interest.

Since the amount of DNA printed per spot on the microarray can vary, RNA species from two different samples are used in the hybridization. This is possible since differences in gene expression between samples (such as when and where the gene is expressed or how it changes across different biological situations) is often what matters most in determining the function of the gene and not the absolute abundance the mRNA transcribed from that gene. By using two different RNA pools, a differential expression pattern is acquired for the genes of interest relative to a control or normal state (12) (Figure 2). The result is a transcription profile of the genes that are upregulated or downregulated in one condition vs. another.

In performing these experiments, two different RNA pools are directly compared by labeling each of them with a spectrally distinct fluorescent dye. The mRNA from each total RNA sample is labeled with a different fluorescent dye in a 1st strand cDNA synthesis reaction (33). The dyes typically used are Cy3-dUTP and Cy5-dUTP because they have good incorporation rates relative to other fluorochromes and are widely separated in their excitation and emission fields by a configured laser scanner (11). The two samples are pooled together and hybridized to the microarray simultaneously. The relative abundance of a gene present in the two samples is assayed by measuring the ratio of the fluorescence intensities of the two dyes present within the cDNA that hybridized to its complementary DNA sequence (or spot) on the microarray (12). This ratio is then

Figure 2.
Scheme for comparing the differential expression level of genes from two different RNA samples using cDNA microarrays.

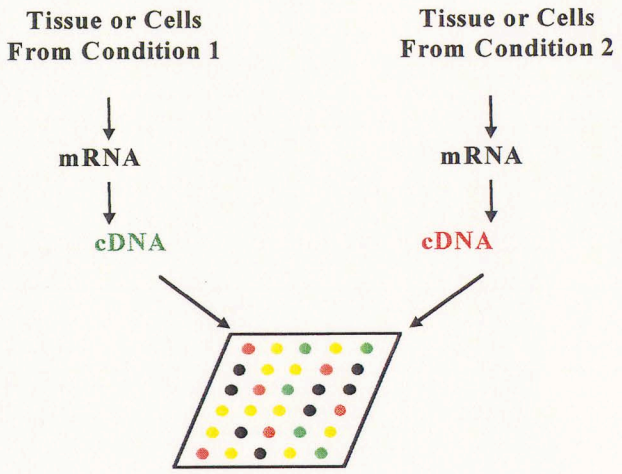

correlated to a fold increase or decrease of a gene between the two samples hybridized. Collectively, genes are then grouped into specific fold change categories and graphed using analysis algorithms such as self organizing maps (SOM's) or cluster analysis in order to elucidate functionality (8) (49).

As mentioned previously, making and using DNA microarrays requires two pieces of hardware. The printing robot (or arrayer) spots the DNA in nanoliter volumes using single or multiple printing tips (9). These printing tips pick up the DNA (suspended in 2X SSC) in a variety of ways, usually via capillary action, from 96 or 384 well microtiter plates and spot the DNA onto the surface of the slides. As many as 100 slides can be made concurrently using this method with the arrayer washing each printing tip before moving on to the next gene (11). The second piece of hardware needed is a microarray scanner, which images the hybridized microarrays (12). The scanner is configured to shine two different wavelengths (or more) of light corresponding to the excitation levels of the fluorochromes incorporated into the cDNA that have hybridized to the slide surface. Currently, many different scanners are commercially available, each having different capabilities and limitations.

Once the hybridized microarray has been imaged, analysis software is needed for gene quantification. The purpose of this software is to reduce an image of multiple spots of varying intensities into a table containing a measure of the ratio of intensities. Although seemingly straightforward, this is more difficult than anticipated (4). Inhomogeneities in the slide surface and background noise brought about by unpurified, labeled cDNA pose problems for reliable results. Additionally, printing integrity and

spot quality from slide to slide is an issue that has yet to be resolved. Many different microarray analysis software packages are currently available through the industry or have been developed privately by individual research labs (4).

In order to fully utilize the tremendous amounts of data that come out of every hybridization, the development of some type of "gene expression data mine" for collecting, storing, querying, and analyzing data is needed as well. Currently, only a handful of research labs have such capabilities and the ability for outside labs to access them are not possible. In order to create this data mine, a data warehouse must first be designed that can integrate studies from all over the world, much like GenBank does for DNA sequences today. The database will steadily build as more and more gene expression studies are performed (4). Construction of such a resource-based warehouse is a difficult process to undertake.

Finally, due to the fact that DNA microarray technology is so new, no set protocols exist for any one step. As noted earlier, many different DNA attachment chemistries are available through the industry as well as printing tips, laser scanners, hybridization chambers, and printers. Additionally, hybridization buffers and conditions, labeling of mRNA with fluorochromes, purification of labeled cDNA, and microarray processing conditions were all components that needed to be resolved as well. For any research lab, these parameters must be optimized.

Overall, as described previously, DNA microarrays are and will continue to be a very powerful tool in looking at the expression levels of mRNA. Recent publications show that the detection limit of DNA microarrays allows for the monitoring of transcripts

present as low as 1:500,000 in the total RNA pool (40). Also, the sensitivity of the microarray system is such that increases or decreases in expression levels as low as two fold are detectable using the two-color fluorescence system. Further studies have shown that absolute mRNA levels detected by DNA microarrays are similar when correlated to Northern Blots, depending on the nature of the experiment (3). Additionally, the expression levels of mRNA with DNA microarrays have been shown to be in agreement with results from in situ hybridization studies (29). This being the case, along with the fact that thousands of genes can be measured differentially at the same time for any biological system, provides solid insight as to why DNA microarrays are so powerful and very useful to labs using molecular or cellular biology for gene expression studies.

The adaptable nature of the fabrication and hybridization methods allows for DNA microarrays to be widely used. By using a BLAST search, base pair sequences for genes of interest or genes similar in sequence to known genes (EST's or expressed sequence tags) can be identified (28). Therefore, the only limitation is the number of sequences available in the database and the strength of the microarray experiments designed relies on the number and particular elements chosen. Thus, biologically complex processes involving the interplay of many genes can be chosen as worthwhile experiments for microarray studies.

ANGIOGENESIS

Angiogenesis is a process by which new vasculature sprouts from quiescent, existing vasculature. It occurs in utero during embryonic and fetal development and in

certain physiological and pathological situations which are accompanied by the abnormal high or deficient growth of new vessels during post-natal life (34) (52). Examples of physiological situations where angiogenesis occurs include the follicle and corpus luteum, in the uterus during ovarian and menstrual cycles, and during pregnancy (34). Pathological situations in which it can occur include wound healing, inflammation, ischemia, and tumor formation and growth (32). Under conditions of reproduction, development, and wound repair, angiogenesis is turned on (regulated) for brief periods of time and then completely inhibited (20). Under other conditions, such as tumor growth, angiogenesis is constantly underway.

The term angiogenesis was first coined in 1935 to describe the formation of new blood vessels in the placenta (19). Since then, many different assays have been conducted to try and identify the angiogenic factors responsible for the sprouting of capillaries. In these in vivo assays, material to be tested is placed in an area that has a low background of pre-existing vessels yet will allow the formation of new capillaries. Among the many areas chosen for study of angiogenesis in the past were the hamster cheek pouch (22), the rabbit ear chamber, the chick choriolallantoic membrane (16) and the rabbit cornea (21).

Currently, angiogenesis is thought to occur in an ordered sequence of events (14). Briefly, the basement membrane surrounding the endothelial cell tube is locally degraded by the release of collagenases and proteolytic enzymes (plasminogen activators) from the microvascular endothelial cells (34). The endothelial cells underlying the degraded cell tube then change shape and invade/migrate to the surrounding stroma by chemotactic

mechanisms. This invasion/migration is coupled by proliferation of the endothelial cells at the leading edge of what becomes the migrating column. Just behind the advancing front, a region of differentiating endothelial cells that are no longer proliferating change shape and tightly adhere to each other to form the lumen. Finally, the sprouting tubes fuse and coalesce into loops, allowing for blood to begin circulation in the newly formed vessels (24) (32) (52).

The complexity of angiogenesis suggests the existence of multiple controls involving many different angiogenic factors. Studies performed on gene knockout mice have shown that vascular endothelial growth factor (VEGF) and its tyrosine kinase receptors Flk-1 and Flt-1 (42) and the activating angiopoetin ligands (23) and their receptors TIE-1 and TIE-2 (38) all produce lethal embryonic phenotypes resulting in defects from angiogenesis (51) (2). Also known to be involved with blood vessel formation are the transforming growth factors (TGF-β1 and TGF-β2) (19), the ephrin ligands B2 and B4 and receptor eph B2 (45), and tumor necrosis factor (TNF-α). Many other classes of molecules may also be involved, including matrix molecules, cell-cell adhesion molecules, cell-matrix adhesion molecules, matrix enzymes, inflammatory genes, endothelial and smooth muscle cell specific differentiation genes, transcription factors, hypoxia induced and apoptosis induced genes (35).

Recent work has emphasized that a genetic switch program exists to regulate angiogenesis. This "angiogenic switch" is thought to involve a shift in the balance of angiogenesis factors and inhibitors. Angiogenesis is quiescent when inhibitors are present in proper amounts and angiogenesis is active when factors are high and/or

inhibitors are low (24). However, the detailed genetic changes and their effects on angiogenesis in physiological situations such as development and pregnancy and in pathological situations such as healing responses and ischemia are poorly understood (6). Because of this, the intent of this study was to use DNA microarrays to observe the expression levels of most of the genes believed to be involved in a controlled angiogenic response in order to elucidate the genetic program used by endothelial cells to achieve this response.

In order to produce an angiogenic environment with which to study, a controlled healing response was created in mice. Sehl *et. al* recently described a process by which controlled reponses to injury can be obtained from rat hearts that produced viable tissue and mRNA samples (41). Furthermore, it has been shown by Williams *et al.* that healing associated with expanded polytetrafluoroethylene (ePTFE) implants in rats is specific to the nature of the porosity or surface modification of the polymer implant (5). Specifically, small pores 30 μm in size contribute to the formation of a fibrous capsule while larger pores of 60 μm in size allow for endothelialization in the subcutaneous region of the rat haunch after five weeks of implantation (36) (37). Also, denucleation (removal of air trapped within the interstices of porous ePTFE) and surface modification of the polymer, such as the deposition of extracellular matrix onto the polymer surface, show the absence of a fibrous capsule and the formation of new blood vessels within and around the ePTFE in rats after 5 weeks (5). More recent results have shown that ePTFE has similar effects in mice. This difference in angiogenic responses based on the

implantation of specific forms of ePTFE provides a good model with which to identify angiogenesis-specific gene expression.

The series of experiments designed for this study utilized the fact that the amount of angiogenesis associated with a wound-healing response can be controlled by the implantation of modified and unmodified ePTFE in the subcutaneous position of the rear haunch in mice. Surface modified ePTFE was manufactured by allowing II-4 cells (a cancerous cell line that exhibits a pro-angiogenic activity) to deposit extra-cellular matrix onto the surface of the polymer in a process called sodding as described by Ahlswede (1). This modified form of ePTFE, when implanted, induces angiogenesis within and around the polymer. Unmodified ePTFE induces low amounts of angiogenesis when implanted and thus serves as a baseline control. By explanting the polymers and the surrounding tissue from the mice, and by hybridizing the labeled mRNA isolated from each sample to a microarray containing many angiogenesis-specific genes, a transcription profile of the genes involved in angiogenesis was obtained. The time point of five weeks was chosen in order to capture the angiogenic profile at the stage when fully developed vasculature is present. The set of genes included on the microarray consisted of many classes of molecules as discussed by Risau *et al.* (35), Folkman *et.al.* (17) (18), Carmeliet *et.al* (6), and Hanahan *et.al* (24) and is shown in Table 1. The set represents all of the genes for mice that have sequence available in GenBank and are considered relevant to angiogenesis.

An additional angiogenic environment used for this study was solid tumors present in the muscle tissue (sarcomas) on the bodies of mice. Tumors provide a good

source of angiogenesis since the main requirement for a tumor to survive and grow beyond a certain size involves a continuous supply of fresh blood and hence the formation of new vasculature (47). Gene expression in such a system is highly uncharacteristic and provides an interesting situation with which to look at gene function and interplay. Additionally, studies have shown that angiogenesis occurs in a growing tumor constantly until the host dies or the tumor is eradicated (15). Thus, inhibition of angiogenesis in a tumor is thought to be a viable approach to therapy for patients suffering from solid tumor growth (26).

Tumor angiogenesis is thought to be induced by a permanent shift in the balance between angiogenic factors and inhibitors. Recent studies suggest that cancer cells, vascular endothelial cells, and other stromal cell types all release angiogenic factors that offset the amount of inhibitors, causing the formation of new vessels (31). However, is it unclear which genes become activated or down-regulated in tumor angiogenesis because the molecular characteristics of such a system are again ill-defined (46). By explanting the tumor and hybridizing its labeled mRNA to DNA microarrays containing most of these angiogenic factors and inhibitors as mentioned before, identification of the core group of genes critical to the formation of the new vasculature may be elicited. Additionally, by comparing the transcription profiles obtained for each of the angiogenesis environments studied, differences in groups of genes upregulated or downregulated should be present, corresponding to the different types of angiogenic responses observed.

MATERIALS AND METHODS

Arrayed Gene Sequences and Control Sequences.

Each of the 58 genes spotted onto the array was mined from the GenBank database (http://www.ncbi.nlm.nih.gov/). The genes were chosen because of their relevance to angiogenesis as implied by the literature. The sequences themselves are all mRNA sequences and constitute either a partial or complete coding sequence of the arrayed gene. They range in length from 600 base pairs to 7000 base pairs. The entire panel of genes is listed in Table I.

The two control genes used were chlorophyll a/b binding protein (GenBank accession number 187D7T7) and plant thioredoxin (GenBank accession number 185N8T7) cDNA from *Arabidopsis thaliana* cloned into Lambda zip-lox vector and propagated in *E.Coli*. Both of these EST sequences are flanked by T7 RNA transcription start sites. The two clones were a gift from Dr. Betsy Pierson from the Department of Plant Sciences at the University of Arizona.

Primers.

Primers for each of the angiogenesis related genes were designed using the Primer 3 program (http://waldo.wi.mit.edu/cgi-bin/primer/primer3.cgi). Each primer was 20 base pairs long and contained a single CG clamp at the 3' end. Each primer set was designed to amplify a region of 300-600 base pairs in length from the more variable 3' region of the mRNA sequence mined for each gene. The primers were obtained from

Table I
Gene List

Angiogenesis-Specific Genes
Angiopoetin-2
Tie-1
Tie-2
VEGF-A
Flt-1
Flk-1
Ephrin-B2
MDK-5
Collapsin-I
Neuropilin-1

Growth Factors
FGF-1
FGF-2
FGFR-2
TGFB-1
TGFB-2
TGFBR-2
Endoglin
sMAD-7

Matrix Molecules
Laminin-5
Collagen-I
Collagen-IV
Thrombospondin-I
Thrombospondix-II
Vitronectin
Fibronectin

Cell-Cell Adhesion
Cadherin-3
Cadherin-VE
Cadherin-N
PECAM
ELAM
ICAM
Connexin 43
CD34

Cell-Matrix Adhesion
Integrin-αv
Integrin-α6
Integrin-B5
Integrin-B1

Matrix Enzymes
MMP-9
TIMP-2
MMP-MT
Stromelysin-I

Transcription Factors
EGR-1
NFkB
ETS-1
Vezf1
GATA-4
Jun
Fos
MEF-2

Endothelial Cell Differentiation
SERCA3
vWf
eNOS
NK-1 receptor

Smooth Muscle Cell Differentiation
α-actin
smooth muscle myosin
SM22α

Inflammation
INOS
IL-1α

Control Genes
Thioredoxin (plant)
Chlorophyll A/B Binding Protein (plant)

Integrated DNA Technologies (http://www.idtdna.com). A complete listing of the primers designed for each gene as well the sequences for the Cy-3 and Cy-5 dCTP positional marker oligos (Integrated DNA Technologies) is listed in Appendix A.

Primers used for the control genes were standard M13 forward and M13 reverse sequencing primers (Integrated DNA Technologies) which recognize sequence flanking each clone. Their sequences are listed below.

M13 Forward: 5'-CCCAGTCACGACGTTGTAAAACG-3'

M13 Reverse: 5'-AGCGGATAACAATTTCACACAGG-3'

PCR Reactions and Components for the 58 genes.

100 µl PCR reactions were performed on each of the 58 genes using PCR programs designed in the lab. The source the PCR template was RNA extracted from a day 7 mouse embryo weighing approximately 300 mg or an adult mouse uterus. The RNA was extracted using the RNAZol B isolation kit (Tel-Test, Inc. Friendswood, Texas) and was converted to 1st strand cDNA using the RT-PCR protocol (Appendix B, protocol 1). A 20 µl pilot PCR reaction was performed to validate the reaction prior to product scale up. Subsequently, 100 µl PCR reactions were performed on each gene (Appendix B, protocol 2). The PCR reactions were run on one of four thermocycler programs named MAGIC-35, MAGIC-42, β-ACTIN, and β-ACTIN-42.

The MAGIC-35 program is as follows:

Step 1: 95° C for 0:01:30
Step 2: 57° C for 0:00:50

Step 3: 72° C for 0:01:30
Step 4: 95° C for 0:00:50
Step 5 Goto Step 2 34 more times
Step 6 59° C for 0:00:50
Step 7 72° C for 0:05:00
Step 8 28° C for 0:10:00
Step 9 End

MAGIC-42 goes to Step 2 41 more times.
β-ACTIN-35 has 59° C for Step 2
β-ACTIN-42 goes to Step 2 41 more times at 59° C in the β-ACTIN program.

Table II shows the list of genes and their corresponding thermocycler programs.

PCR reactions for the control clones.

The 2 control clones were grown up overnight in 5 ml LB media broth containing 5 µl ampicillin (50 mg/mL). Subsequently, the *E Coli* were lysed and the plasmids were isolated using the QIAGEN Miniprep Kit. Purified plasmids were then diluted 100 fold and 5 µl was used in a 100 µl PCR reaction in place of the cDNA template. The control products were generated with the MAGIC-35 program using the M13 forward and reverse primers.

Electrophoresis of the PCR products.

All 58 genes and the two control genes were run on horizonatal slab 1.2% agarose gels in TAE buffer (40.0 mM Tris-HCl and 5.0 mM NaOAC) to check for proper size. 2 µl of ethidium bromide (10 mg/mL) was added to each gel for staining purposes. 5 µl of

Table II
Master PCR Program List

MAGIC-35	MAGIC-35	B-Actin
TIE-1	Collagen-4	VEGF-A
TIE-2	Thrombospondin-1	Collagen-1
Integrin-A6	Thrombospondin-2	CD34
Endoglin	TIMP-2	Collapsin
Integrin-B1	Fibronectin	SMC-myosin
Integrin-AV	Fos	MDK5(uterus cDNA)
ANG-2	eNOS	PECAM
SMCα–Actin	Jun	
Vwf	IL-1α(uterus cDNA)	
INOS	GATA-4	**B-Actin-42**
FLT-1	MEF-2	
Vezf1	Neuropilin	Stromelysin-1
TGFB1	MTMMP	
TGFB2	MMP-9	**MAGIC-42**
sMAD-7	Ephrin-B2	
SM22α	Vitronectin	Laminin-5
TGFBR2	CHLORO	
Cadherin-N	THIO	
Cadherin-VE		
Integrin B5		
Connexin43		
NK-1 Receptor		
SERCA3		
ETS-1		
FGF-1		
FGF-2		
FLK-1		
Cadherin-3		
EGR-1		
ELAM-1		
FGFR-2		
ICAM		
NFkB		

each PCR reaction was added to each well and the gels were visualized under longwave UV light.

PCR Product and Control Purification.

PCR products were purified by adding ½ volume 8 M ammonium acetate and 2 ½ times volume 100% pure ethanol. The products were stored at –80° C for 1 hour and pelleted at 4° C (max. speed, 15 min.) using a Beckman tabletop centrifuge and washed with 200 µl 70% ethanol (max. speed, 5 min). The products were resuspended in 2X SSC (17.5 g 3 M NaCl, 8.8 g 0.3 M Na_32H_20, 100 ml H_20) at a final concentration of 3 µg/10 µl.

Sequencing of Generated PCR Products.

PCR products from ten genes were sequenced using the DNA sequencing center at the University of Arizona. 5 µl samples were submitted at 200 ng/ml and results obtained were verified against the GenBank sequences.

Coating of Slides.

5 slide chemistries were identified for this study: 2 silylated epoxides, 1 commercial coating (CEL) and 2 proprietary epoxides from S2. Epoxide slide I was made with 3-(2,3-Epoxypropoxy)propyltrimethoxysilane (Gelest, CO) and is shown in Fig 3a. Epoxide slide II was made with 2-(3,4-Epoxycyclohexyl)ethyltrimethoxysilane (Gelest, CO) and its structure is shown in Fig. 3b. Slides from CEL and S2 were

Figure 3.
Non-commercial slide chemistries (epoxides) coated in the lab for comparison against commercial products.

a) Chemistry for epoxide coating I:
3-(2,3-Epoxypropoxy)propyltrimethoxysilane

b) Chemistry for epoxide coating II:
2-(3,4-Epoxycyclohexyl)trimethoxysilane

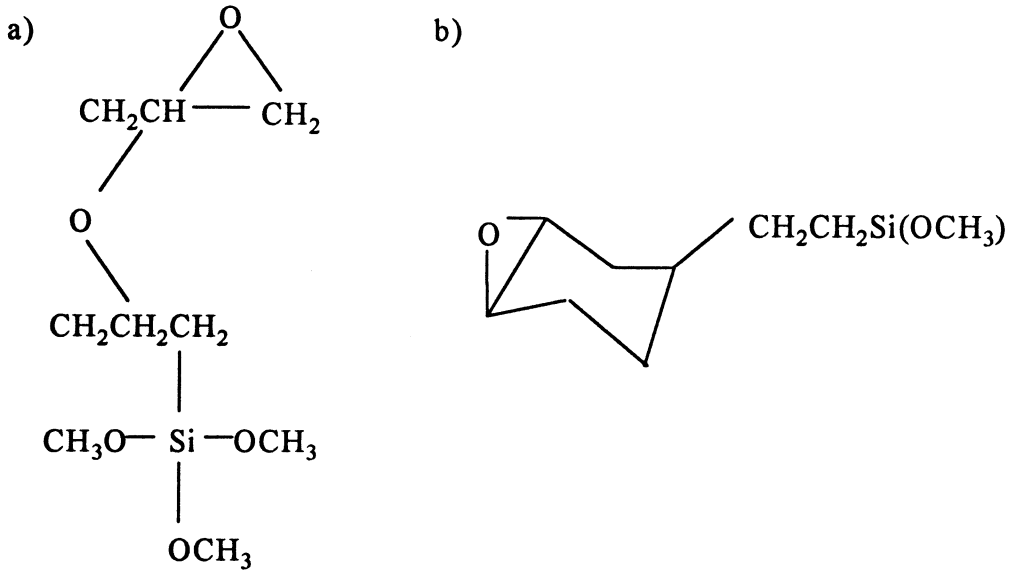

supplied precoated. The two epoxide coatings were applied in the lab. Solutions containing each of the above epoxides were made by diluting 7-ml of the respective epoxide in 350 ml of a 99% hexane solution (Aldrich) for a 2% final cocnetration in a glass-staining jar. Three separate glass staining jars containing 350 ml of a 99% hexane solution were set-up next to the 2% epoxide/hexane solution. 100 pre-cleaned glass premium microscope slides (Fisher) were wiped clean with a static free rag and placed into 30 well metal slide racks. Slides were coated in a fume hood by first prewashing in 99% hexane solution for 2 minutes and followed by transfer to the 2% epoxide/hexane solution for 5 minutes. Slides were immediately transferred to a clean 99% hexane wash, submerged for 2 minutes, and washed again in another clean 99% hexane bath for 2 minutes. The slide rack was removed and allowed to dry overnight in the hood. Slides were covered with tin foil while drying to avoid settling dust. Care was taken to make transfers between baths quickly to prevent evaporation and thus keep down background fluorescence. At first, 30 slides of a coating were prepared for pilot tests. For the final printings, 120 slides were coated at once to improve homogeneity in coatings. Cost of producing each of these slides was about $0.80 per slide.

Printing of Arrayed Genes.

Two sets of microarray printings were performed using a robotic printer (GeneMachines) available at the Plant Sciences Department at the University of Arizona. The first print involved spotting 10 genes in duplicates and also included 2 amino-modified genes Integrin-β1 and TIE-2, which contained 5' amino-modified endgroups

(Integrated DNA Technologies). Additionally, a dilution series from 1/10 to 1/100000 the normal concentration (3 μg/10 μl) of the gene Integrin-β1 and amino-modified Integrin-β1 were printed to test attachment strengths. Finally, a control gene (Flt-1 from rat) and a short oligomer containing the fluorescent nucleotide Cy-3 dCTP (Amersham) at 10 μM in 2X SSC were printed for a cross-hybridization and positional marker respectively. The genes were arrayed onto 5 different slides coated with Sigma I, Sigma II, CEL, Epoxide I and Epoxide II. The genes were printed with one Telechem ChipMaker 2 Micro Spotting Pin (ArrayIt) in the presence of ambient humidity from a 96 well microtiter plate from 10 μl samples. Each spot on the array contained ~1 nl of liquid and the total print time was 4 hours. Spacing between each spot was 750 μm and spot size was 100 μm. The layout of the prototype microarray is shown in Fig. 4. Slides were stored in plastic slide cases at room temperature in the dark until use. These slides were used to test slide coatings and demonstrate proof of principle (see results page 52-53).

The second print (or "Big-Array") involved arraying 58 angiogenesis genes plus the 2 plant controls. Each gene was spotted in triplicate in 1 nl spots in a predetermined grid using one ChipMaker 2 Microspotting Pin. A total of two complete microarrays (Fig. 5) were printed on 88 slides of the chosen chemistry (Epoxide I), ten poly-l-lysine slides and 2 CEL slides. The printing was performed at 25% humidity and the genes were organized into a 96 well microtiter plate in 10 μl samples at a concentration of 3 μg/10 μl. The total print time was 2 hours. Cy-3 and Cy-5 labeled oligomers (10 μM in 2X SSC) were spotted at the corners of each array for visualization

Figure 4.
Prototype microarray layout for the five slide chemistries printed on.

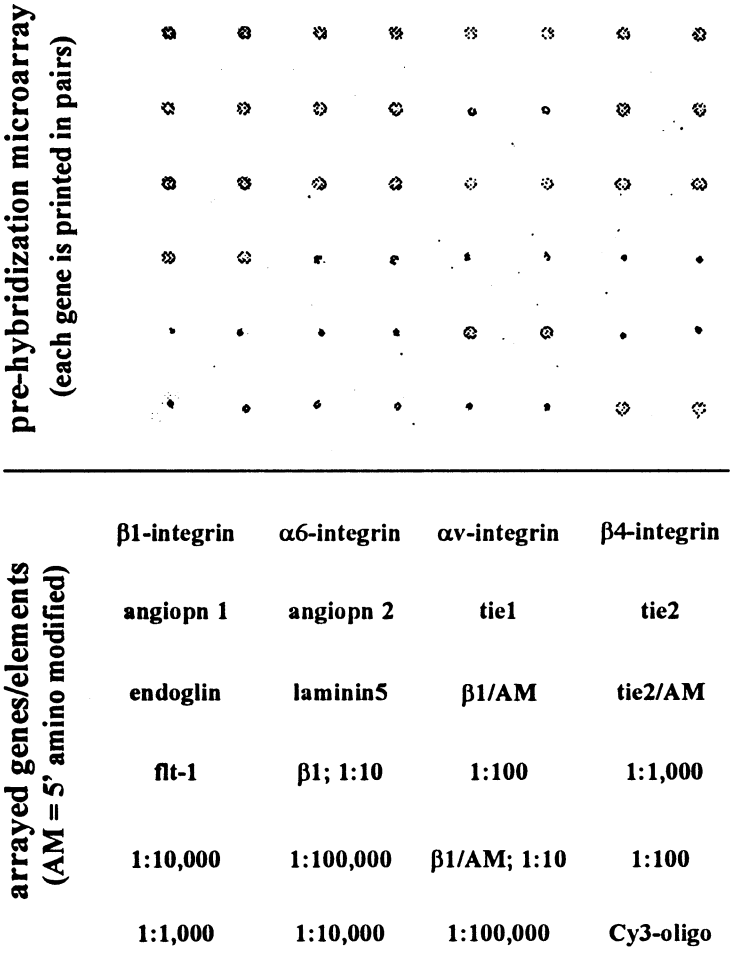

Figure 5.
Layout of Big-Array.
Each set of three dots represents 1 gene printed in triplicates.

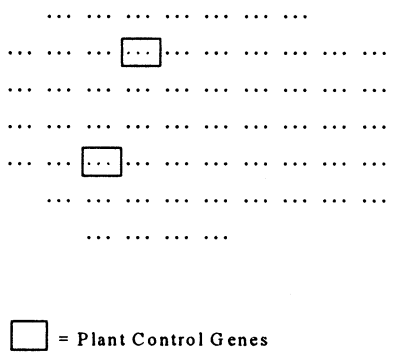

purposes. The spacing between each spot was 250 μm and spot size was 100 μm. Slides were stored in the desicator at room temperature until use.

Processing of Microarrays.

Microarray slides were rehydrated (DNA side down) in horizontal 50 ml Falcon tubes containing 1 ml ddH_20 for 5 minutes at room temperature. The slides were then snap dried (DNA side up) on a 75° C hotplate for 3 seconds. Arrayed elements were circumscribed with a diamond scriber and the entire slide was blocked in 30 ml of a fresh sodium borohydride solution (1 g $NaBH_4$, 100 ml 100% ethanol, 300 ml PBS) for 15 minutes at room temperature in a staining jar on an orbital shaker. The slides were then submerged in 95° C ddH_20 for 2.5 minutes, plunged into cold 100% ethanol for 15 seconds and dried by centrifugation (700 rpm) in vertical 50 ml Falcon tubes for 5 minutes. The microarrays were stored in a desicator at room temperature until ready for use.

II-4 Treatment of ePTFE.

Confluent cultures of II-4 cells were sodded onto expanded polytetrafluroethylene (ePTFE) polymer stock (IMPRA Inc.), 4 mm internal diameter, 30 μm internodal distance, standard wall, and 5 cm in length. Cultures were trypsinized (trypsin/EDTA) and suspended into medium (Dulbecco's Modified Eagle Medium high glucose, 10% Fetal Bovine Serum, 2mM L-Glutamine, and 5 mM HEPES buffer). The cell volume

required to coat the luminal surface of the polymer with 2 x 10^5 cells/cm^2 was calculated and the cells were pressure sodded onto the luminal surface of the ePTFE and grown in culture medium for 8 days. Cells were removed from the ePTFE with 40 mM ammonium hydroxide for 1 hour with solution changes every fifteen minutes. Following cell removal, the ePFTE was rinsed 3 times with di-cation free phosphate buffered saline (DCF-PBS). The II-4 cell line was a generous gift from the lab of Dr. Ray Nagle in the Department of Pathology at the University of Arizona. Treatment of the polymer stock was performed by Kameha Kidd in the lab of Dr. Stuart Williams in the Department of Biomedical Engineering at the University of Arizona.

Polymer Implants.

Eight mice from the 129-SVJ strain were obtained from Jackson Labs and were used for this study. All of the mice were male and between the ages of 6-8 weeks. Four baseline mice were implanted with unmodified expanded polytetrafluoroethylene (ePTFE) and four mice were implanted with II-4 modified ePTFE. Each of the baseline mice were implanted with two 6 mm^2 unmodified ePTFE discs and one 4 mm^2 unmodified ePTFE disc in the subcutaneous position of the rear haunch. Four experimental mice were implanted with two 4 mm^2 II4-modified ePTFE discs and one 6 mm^2 II-4 modified ePTFE disc in the subcutaneous region of the rear haunch. Mice were anesthetized with 0.15 ml of 2.5% Avertin per 10 g of body weight and 3 incisions were made with a scalpel per mouse in the rear haunch position. One polymer disc was placed into each incision (3 per mouse) and the skin was fastened shut with a metal clamp.

These implantations were performed by the Williams lab. A chart of all mice implants is listed in Table III.

Mouse Tumors.

Mammary tumor cells from the cell line EMT6 were injected at two different points the subcutaneous region of the rear haunch of 6 a six week old mouse. Tumors were allowed to grow until they had achieved a size of 0.5-1 cm in diameter. These tumors were a gift from the lab of Dr. Emmanuel Akaporiaye in the Department of Cancer Biology.

Tumor/Polymer Explants and Tissue Preparation.

Polymer explants were performed at 5 weeks post-implantation according to the chart. At explant, mice were again anesthetized using 0.15 ml of 2.5% Avertin per 10 g of body weight. The entire polymer and its surrounding tissue to be hybridized to the microarrays were explanted, placed into labeled 6 ml cell culture tubes, and immediately frozen in liquid nitrogen to protect the RNA from degradation. Subsequently, the tissue was stored at –80° C until use.

For removal of the tumors, the mouse was anesthetized using Avertin as described above. Both tumors were excised in their entirety, placed into a 6 ml cell culture tube, and immediately frozen in liquid nitrogen and stored at –80° C until use.

Table III
Mouse Implant Chart

Mouse #	Sample	Number of Implants	Date of Explant	Sample for Histology
92	II-4	2-4mm 1-6mm	2/15/00	1/2 6mm
91	II-4	2-4mm 1-6mm	2/15/00	1/2 6mm
90	II-4	2-4mm 1-6mm	2/15/00	1/2 6mm
89	II-4	2-4mm 1-6mm	2/15/00	1/2 6mm
85	control	2-6mm 1-4mm	2/15/00	1/2 6mm
84	control	2-6mm 1-4mm	2/15/00	1/2 6mm
82	control	2-6mm 1-4mm	2/15/00	1/2 6mm
81	control	2-6mm 1-4mm	2/15/00	1/2 6mm

Preparation of Labeled Probe.

PCR products were amplified in the presence of 1 mM Cy-3 dCTP and Cy-5 dCTP fluorochromes in 20 µl PCR reactions (Appendix B, protocol 3). Each of these reactions was run on the thermocycler program MAGIC-35. RNA was extracted from the healing tissue by re-freezing the tissue in liquid nitrogen and then crushing it (along with the polymer) into a fine powder using a mortar and pestle. The RNA was extracted from this fine powder using the RNAzol B protocol (Tel-Test, Inc.). The RNA was then labeled in a first strand cDNA synthesis reaction in presence of 1 mM Cy-3 dCTP or Cy-5 dCTP (Appendix B, protocol 4).

Purification of Labeled Probe.

Labeled PCR products were purified using G-50 microspin columns (Amersham) to remove unbound nucleotodies. The PCR products were concentrated by adding ½ volume 8 M ammonium acetate and 2 ½ times volume 100% ethanol and then by storing the mixture at –80° C for 1 hour. The PCR products were pelleted at 4 C (max. speed, 15 min.) using a Beckman tabletop centrifuge. Pellets were washed with 200 µl 70% ethanol (max. speed, 5 min.) and resuspended in 2 µl sterile TE (Tris-EDTA) buffer and 10 µl PerfectHyb Plus Hybridization Buffer (Sigma).

Labeled cDNA was purified by adding 1 µl 1% SDS (1 g SDS in 1 Liter H_20), 1 µl 0.5M EDTA (18.61 g $Na_2EDTA\ 2H_20$, 100 ml H_20, pH-8), and 3 µl 3 M NaOH. The mixture was stored at 68° C for 15 minutes, equilibrated at room temperature for 15 minutes, and neutralized by adding 10 µl 1 M Tris-HCl (121 g Tris-base, 800 ml H_20,

pH-7). Labeled cDNA's were then combined and purified again by spinning through two G-50 microspin columns to remove all remaining unbound nucleotides. The combined cDNA's were concentrated by adding ½ volume 8 M ammonium acetate and 2 ½ times volume 100% pure ethanol. The products were stored at –80° C for 1 hour and pelleted at 4 C (max. speed, 15 min.) using a Beckman tabletop centrifuge and washed with 200 µl 70% ethanol (max. speed, 5 min). The pellets were resuspended in 1 µl sterile TE and 12 µl PerfectHyb Plus Hybridization Buffer (Sigma).

Hybridization of Microarrays.

Labeled probes were prepared for hybridization by adding 1 µl of CoT-1 DNA (10 mg/ml), 1 µl poly dA oligo (8 mg/ml), and 1 µl yeast tRNA (4 mg/ml) to each sample which were used as blockers. The entire solution was heated for 2.5 minutes at 95° C and placed on ice for 30 seconds. The hybridization chamber (ArrayIt) was prepared by positioning a post-processed microarray slide in it and adding 20 µl dH_20 to each well. Labeled probe was then applied to the microarray slide and a glass cover slip (22 x 22 mm) was placed on top of it. The hybridization chamber was then sealed and submerged in a 62° C water bath for 15 hours.

After hybridization, the microarray slides were washed in 200 mL 1X SSC/0.03% SDS solution for 5 minutes on a horizontal shaker. The microarrays were then immediately transferred to 200 mL 0.2X SSC solution and washed for 5 minutes on a horizontal shaker. Finally, microarray slides were transferred to 200 mL 0.05X SSC and

washed for 5 minutes. Slides were then dried by centrifugation (700 rpm) for 5 min. in vertical 50 ml Falcon tubes.

Scanning of Hybridized Microarrays.

Microarrays were scanned using the ScanArray 3000 (GSI Lumonics) at the Plant Sciences Department. Initially, 50 μm quick scans were performed to locate the microarrays on the slide. Then, the microarrays were scanned at 10 μm spatial resolution for each channel (Cy-3 and Cy-5). For both scans, the setting for PMT (percent maximum threshold) was 85% and the laser intensity was 90%. Images were saved as tiff files on zip disks and later transferred to CD using a CD burner in morphology (room 5305, Department of Biomedical Engineering).

Analysis of Hybridized Microarrays.

Analysis of hybridized microarrays was performed by using the ScanAlyze software available at http://cmgm.stanford.edu/pbrown/. The gain was set to 4 and the norm was set to 1 on the initial setting screen. An overlayed image (in the form of a bit map file) for visual purposes was then created after the *redraw* key was selected for each microarray scanned. A computer grid containing the exact number of spots present on the hybridized microarrays was formed that fit on top of the redrawn overlaid image by selecting *new grid* from the options. This step was performed once and the grid was saved as a SAG file (ScanAlyze Grid File) and reused for each subsequent microarray since the same microarray in the same pattern was printed on each slide. Each grid was

designed with 250 μm spacing between spots and rows and the spot size was set at 12 pixels by 12 pixels (each pixel equals 10 μm which was the resolution of the scan used). The grid was adjusted on a spot by spot basis so as to completely enclose the microarray hybridization spot into each circle present within the grid. Hybridization spots were adjusted by first selecting a spot using the shift and mouse keys and then by using the *warp* and *tilt* options. Once the grid was in place over each spot, the data was saved as a data file and transferred to a Microsoft Excel spreadsheet.

Ratios of gene expression for each spot were calculated by using the following formulas by ScanAlyze:

Adjusted Intensity of Cy-3 = (Cy-3 spot intensity – Cy-3 median background)

Adjusted Intensity of Cy-5 = (Cy-5 spot intensity – Cy-5 median background)

Expression Ratio/gene = (Adjusted Intensity Cy-5/Adjusted Intensity Cy-3)

The expression ratio/gene was taken to be a fold increase or decrease of that gene between each sample. The median background was used because it is lower in value than the mean background. The mean background incorporates the overall background pixel intensity including dust and noise while the median background does not. Thus, the data set is skewed in favor of the mean in terms of values assigned. The background measurement was taken to be the area just outside each circle for each gene defined by the grid. Hybridization signals greater than the background plus 1 standard deviation of the background were considered significant.

Spot quality was determined using the Komolgorov-Smirnov test which comes with ScanAlyze. This test removed spots from consideration that were fluorescing with intensity due to dust particles or noise erroneously placed (i.e. 1 or 2 pixels fluorescing brightly within an area where a spot should be and giving the impression that a spot is present). The test removed these spots from consideration by performing a statistical analysis that assigned a probability factor that there was a difference in intensity between where a spot should be and where the spot should not be (i.e. the values for the background within a particular spot on the microarray). Probability factors greater than 1 x 10^{-4} were not considered while probability factors less than 1 x 10^{-4} were considered as spots for most hybridizations. A Komolgorov-Smirnov value of greater than 1x 10^{-4} means the probability that the distribution between pixel sets within a grid spot is the same is high and thus there is no hybridization (i.e. there was no difference in pixel intensity between the background and the possible hybridization spot). A Komolgorov-Smirnov value less than 1 x 10^{-4} means that the probability that the distribution between pixel sets within a grid spot is the same is low and thus there is a hybridization present (i.e. there was a difference in pixel intensity between the background and the hybridization spot). Additionally, greater than 50% of the six spots of each gene arrayed (two full arrays, triplicates each array) needed to pass the above tests to be considered a usable spot. Thus, hybridization intensity values of each gene were taken to be the average value across the amount of spots passing the tests.

Normalization of the two channels (Cy-3 and Cy-5) was performed by obtaining an average correlation number from the pixel ratios of genes that exhibited no change in

ratio across the two samples compared. These genes were considered housekeeping genes that were expressed in equal amounts between the RNA pools studied. The pixel by pixel ratio for these unchanged genes was written as:

Adjusted Cy-5 Intensity Average /Adjusted Cy-3 Intensity Average

Or

Adjusted Cy-3 Intensity Average/Adjusted Cy-5 Intensity Average

depending on which way the overall signal intensities on the microarray favored. Equal amounts of Cy-3 and Cy-5 fluorochrome produce different intensities of fluorescence depending on laser intensities, scanning properties, and the molar absorbances and qunatum yields of Cy-3 and Cy-5 molecules themselves. Therefore, intensities of one channel obtained on each microarray were either divided or multiplied by the normalization factor, depending on the pixel by pixel ratio calculated by the program. The normalization factor varied between slides and thus changed value for each microarray hybridization. This is because some variability exists between each microarray hybridization due to kinetic issues and pipetting issues.

Using graphs, a quantitative organization of genes from highest to lowest in fold change was designed for each implant (II-4 modified ePTFE vs. unmodified ePTFE) at the 5 week time point. The same type of graph was created for the tumor/normal tissue hybridization experiment. Genes exhibiting a ratio of >1.5 times the amount of mRNA transcript present (or 0.5 fold increase) were considered to be upregulated and significant.

Genes exhibiting a ratio of <1.5 (or less than 0.5 fold change) were not considered to be changed since the sensitivity of microarrays has been shown to be about 1 fold.

RESULTS

Microarray Elements are of Proper Size and Good Quality.

Each of the ten PCR products arrayed onto the prototype microarrays were run out on 1.2% agarose gels to verify the PCR amplification protocols developed. All products amplified on their respective programs did not contain any non-specific products and had the proper base pair length. An example of a gel containing three prototype microarray genes Integrin-B1, Integrin-αv, and Angiopoetin-2 is shown in Fig. 6. In addition to agarose gel electrophoresis, each of the PCR products for the ten prototype microarray genes was sequenced by first pass at the DNA sequencing center located on the campus of the University of Arizona. Each sequenced PCR product had the correct base pair length and was of good quality (i.e. a sequence containing the proper number of base pairs and few ambiguities). Optimal nucleotide alignment comparisons of the sequenced PCR product to sequences in GenBank were also performed. Every analyzed element matched the appropriate gene to within 95% homology. The remaining 5% variation was due to ambiguities in the measured sequence. An example of the optimal nucleotide alignment comparison for the Angiopoetin-2 element is shown in Fig. 7.

For the remaining 48 elements and two plant control elements printed on the Big-Array, each was amplified by PCR in a 100 μl reaction and quality checked by gel electrophoresis. Each of the 48 PCR products corresponding to one gene was run out on a 1.2% agarose gel. An example of a group of genes run on the MAGIC-35 PCR

Figure 6.
1.2% agarose gel of three prototype microarray genes: Integrin-B1 (lane 4), Integrin-αv (lane 5), and Angiopoetin-2 (lane 6).

Figure 7.
Nucleotide optimal alignment of the PCR product angiopoetin-2 vs. the actual sequence of mouse angiopoetin-2 showing a 95.49% match of the base pairs.

```
ANG2actual vrs ANG2PCRsequenced

 165        GCAAGTTTGCTGAACTCACAG-TTTAGAACCCAAAAAGAGA   204
 1          GCANGNTCGCTG-NCTNACANTTTTACAACCCAANANGAGA   40
            *** * * ****  ** ***  **** ******* * ****
GAGAGAATGTGGCAGATCATTTTCCTAACTTTTGGCTGGGATCTTGTCTTG   255
GATANAATGTGGNNAATCATTNTCCTAACTTTTGGCTGGGATCTTGTCTTG   91
** * *******   ****** ****************************
GCCTCAGCCTACAGTAACTTTAGGAAGAGCGTGGACAGCACAGGCAGAAGG   306
GCCTCAGCCTACAGTAACTTTAGGAAGAGCGTGGACAGCACAGGCAGAAGG   142
**************************************************
CAGTACCAGGTCCAGAACGGACCCTGCAGCTACACGTTCCTGCTGCCGGAG   357
CAGTACCAGGTCCAGAACGGACCCTGCAGCTACACGTTCCTGCTGCCGGAG   193
**************************************************
ACCGACAGCTGCCGATCTTCCTCCAGCCCCTACATGTCCAATGCCGTGCAG   408
ACCGACAGCTGCCGATCTTCCTCCAGCCCCTACATGTCCAATGCCGTGCAG   244
**************************************************
AGGGATGCACCCCTCGACTACGACGACTCAGTGCAAAGGCTGCAGGTGCTG   459
AGGGATGCACCCCTCGACTACGACGACTCAGTGCAAAGGCTGCAGGTGCTG   295
**************************************************
GAGAACATTCTAGAGAACAACACACAGTGGCTGATGAAGCTGGAGAATTAC   510
GAGAACATTCTAGAGAACAACACACAGTGGCTGATGAAGCTGGAGAATTAC   346
**************************************************
ATTCAGGACAACATGAAGAAGGAGATGGTGGAGATCCAACAGAATGTGGTG   561
ATTCAGGACAACATGAAGAAGGAGATGGTGGAGATCCAACAGAATGTGGTG   397
**************************************************
CAGAACCAGACAGCTGTGATGATAGAGATTGGAACCAGCTTGC-TGAACCA   611
CANAACCAGACAGCTGTGATGATAGAGATTGGAACCAGCTTGCTTGAACCA   448
** ************************************* *******
GACAGCAGCAC-AAACT 627
GACAGCAGCACAAAANT 465
*********** *** *
 445 Matches over 466 Positions  95.493564%
```

program is shown in Fig. 8a. For elements giving a weak product, such as Interleukin-1α (Fig. 8a, lane 11), an additional 100 μl PCR reaction was performed to increase the total amount of the product for printing. Fifty of the 58 PCR reactions (86%) run exhibited a single band of expected size. The elements for PECAM (lane 8), VEGF-A (lane 9), and CD34 (lane 10) shown in Fig.8b all had additional products that were not removed. Additional elements exhibiting multiple bands were TGFBR-2, ELAM-1, MDK-5, and Stromelysin. Thus, these genes were arrayed with the potential to detect more than one expressed gene. However, it seems likely that these multiple bands might represent isoforms of the same gene, since each of these genes come from families known to have multiple isoforms.

Epoxide I is Comparable to the Commercial Slide Products.

In order to assess which slide chemistry produced the best signal to noise ratio for the lowest cost, prototype microarrays were printed on 5 different slide chemistries consisting of three commercially available products (CEL, S1, and S2) and two epoxide slide coatings identified by the lab. In order to compare the slides to each other, PCR products from Integrin-β1, Integrin-αv, and Integrin-β4 cDNA's were synthesized in the presence of Cy-3 or Cy-5 dCTP according to the protocol shown in Appendix B. By labeling PCR products, the amount of labeled DNA to be applied to the microarray will be in excess to the amount of DNA arrayed on the slide surface. Integrin-β1 PCR products were amplified with both fluorochromes. Integrin-αv was labeled with Cy-3

Figure 8.
Electrophoresis of PCR products from genes run on a) MAGIC-35 and b) β-Actin thermocycler programs.

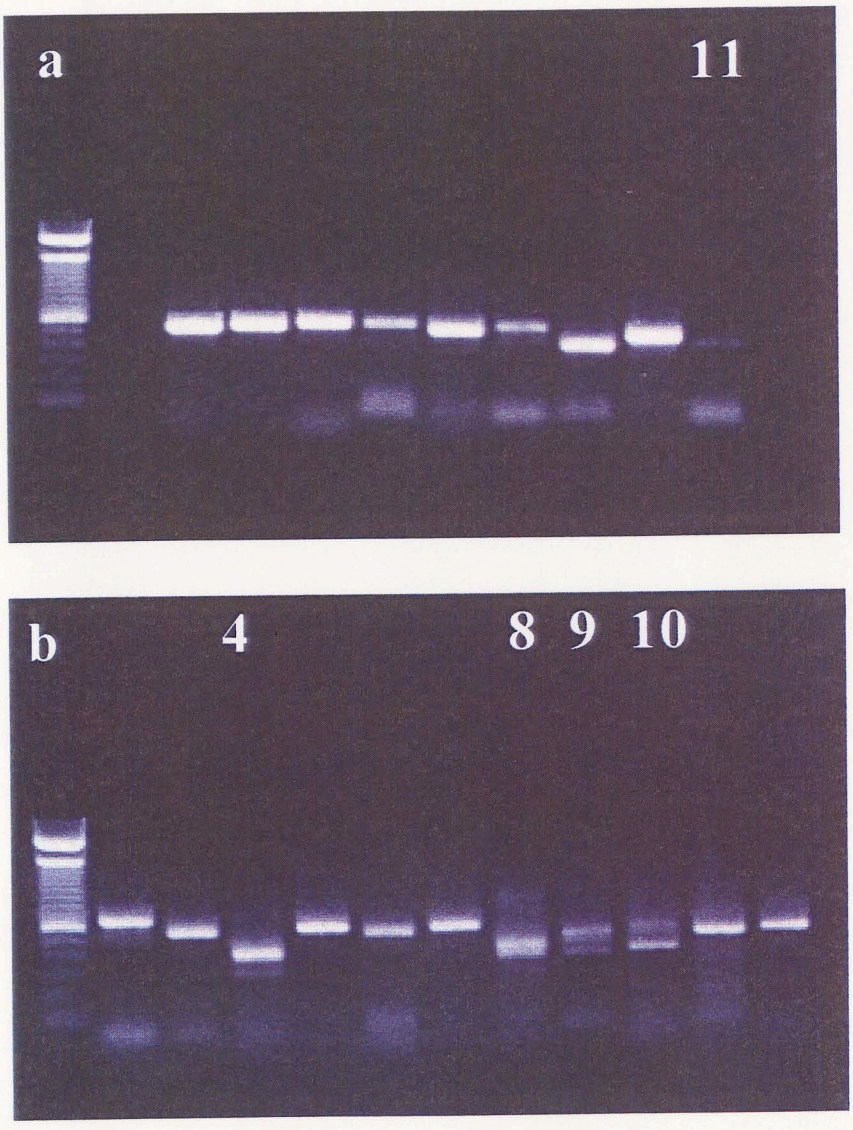

and Integrin-β4 was labeled with Cy-5. Equal amounts of these PCR products (~1 μg) were hybridized to separate microarrays made from each of the 5 slide chemistries. The microarrays were scanned at 10 microns with a laser intensity of 90% and a PMT of 85%. S1 and epoxide II were extremely noisy and exhibited no hybridization signals. As expected, Integrin-β1 appeared yellow since equal amounts of Cy-3 and Cy-5 PCR product was hybridized, Integrin-αv appeared red (Cy-3 only), and Integrin-β4 appeared green (Cy-5 only). In addition, hybridization signals were present for the Integrin-β1-amino modified spots, as well as the 1/10 dilution spots of Integrin-β1 and Integrin-β1-amino modified. No cross hybridizations to other elements were evident. An example of a hybridization experiment to prototype microarray 95 (CEL) is shown in Fig. 9.

Next, particular ratios of labeled PCR products for elements selected on the prototype microarrays were prepared in order to test the accuracy of each microarray type. Integrin-αv was mixed in a 16:1 ratio in favor of Cy-5, Tie-2 was mixed 8:1 in favor of Cy-5, Integrin-β1 was mixed 4:1 in favor of Cy-3, and Endoglin was mixed 2:1 in favor of Cy-3. These mixtures were combined and hybridized to each of the microarrays prepared for the 5 different chemistries. Again, the slide coatings that gave a proper fold change pattern presented by the labeled PCR products were the CEL, S2, and epoxide I chemistries. S1 and epoxide II produced too much noise and had no visible hybridization signals. Hybridization signals were analyzed using ScanAlyze, and the results compared to the expected values. In all but one case, ratios detected by the microarrays were very similar to the expected values. One of the elements for Integrin-

Figure 9.
Visual image of prototype microarray 95 showing equal amounts of Integrin-B1 labeled with Cy-3 and Cy-5 (yellow), Integrin-αv labeled with Cy-3 only (red), and Integrin-B4 labeled with Cy-5 only (green).

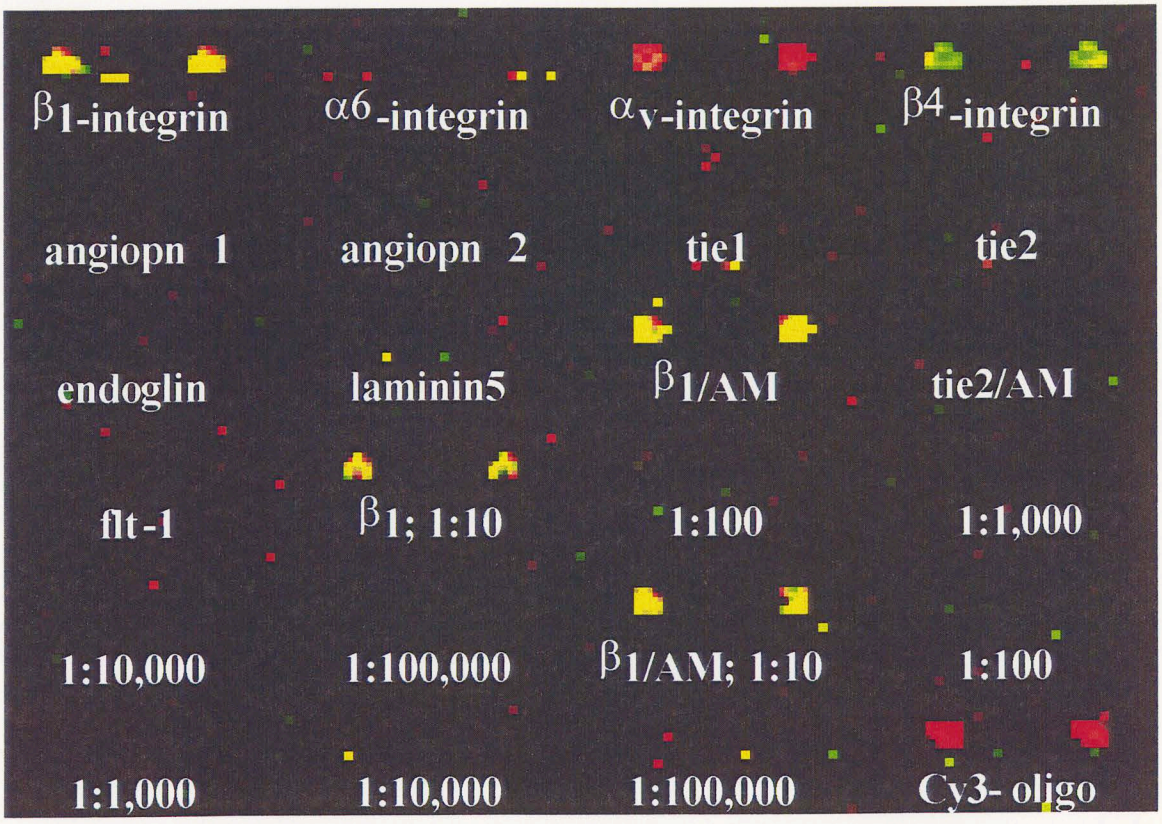

-αv exhibited an erroneous ratio. Visible inspection of that element after hybridization revealed an incomplete spot. Later studies revealed the importance of spot quality in producing accurate results (see discussion). A graph of prototype microarray 27 (epoxide I) intensities and ratios is shown in Fig. 10.

Raw background and hybridization signal intensities from these experiments were compared between the three working chemistries (CEL, S2, and epoxide I). Raw hybridization intensities between the three different slide chemistries were similar for each of the hybridized elements. One exception, the amino-modified Integrin-β1 element, exhibited higher hybridization signal on CEL than for S2 and epoxide I. A graph of the raw hybridization intensities for prototype microarrays 6 (CEL), 25 (epoxide I), and 42 (S2) is shown in Fig. 11. In contrast, raw background signals were remarkably lower for the epoxide I than for the other two coatings (Fig. 12). The value for the background of epoxide I was on the order of 5 times less than CEL and 10 times less than the S2. Due to these results, all remaining hybridizations performed for this study were done with the epoxide I slides.

Quality Control Check of the PMT and Laser Settings Used for the Scanner.

In preliminary experiments, it became evident that the scanner settings used to image hybridized microarrays were important for obtaining reliable data. To determine the proper PMT (percent maximum threshold of the detectors) and laser intensity settings, adjustments to both parameters were made during the scanning of the hybridizations on the prototype microarrays. Laser intensity was decreased incrementally

Figure 10.
Results of fold-change expression pattern for PCR products hybridized to prototype microarray 27. The lines represent intensity of the signals and the bars represent fold changes.

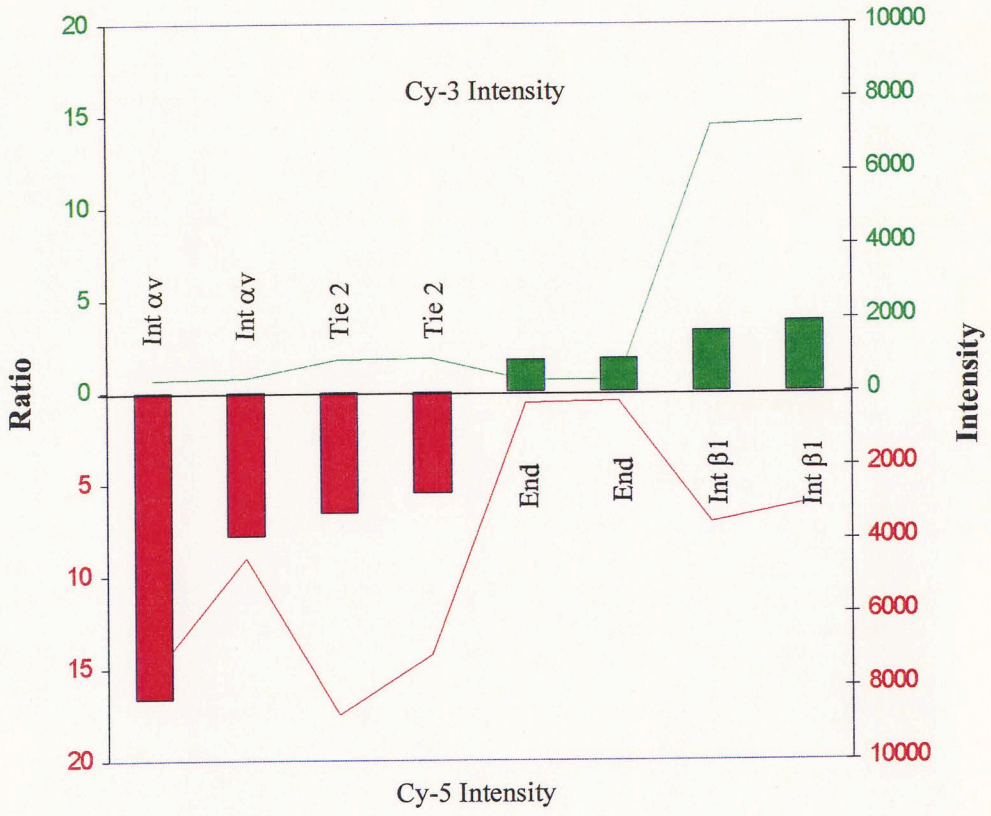

Figure 11.
Raw hybridization intensities of PCR products on prototype arrays for three slide chemistries: array 6 (CEL); array25 (epoxide I); array 42 (S2).

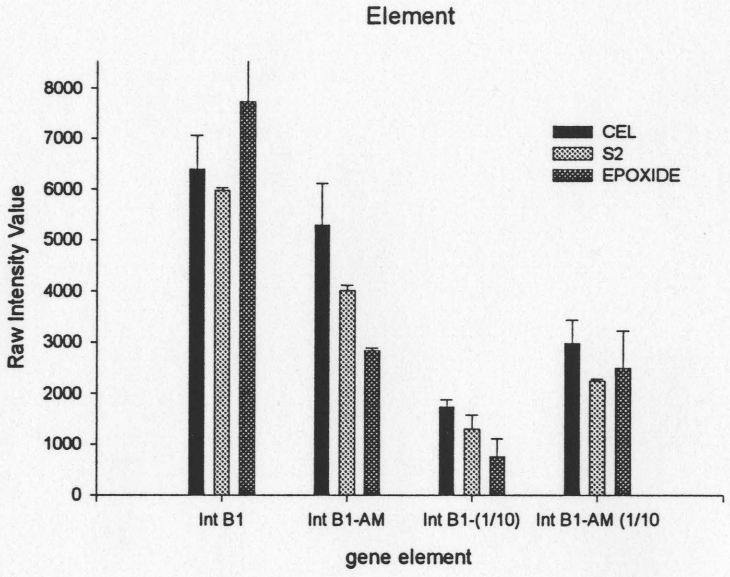

Figure 12.
Raw median background intensities of PCR products on prototype arrays for three slide chemistries: array 6 (CEL); array 25 (epoxide I); array 42 (S2).

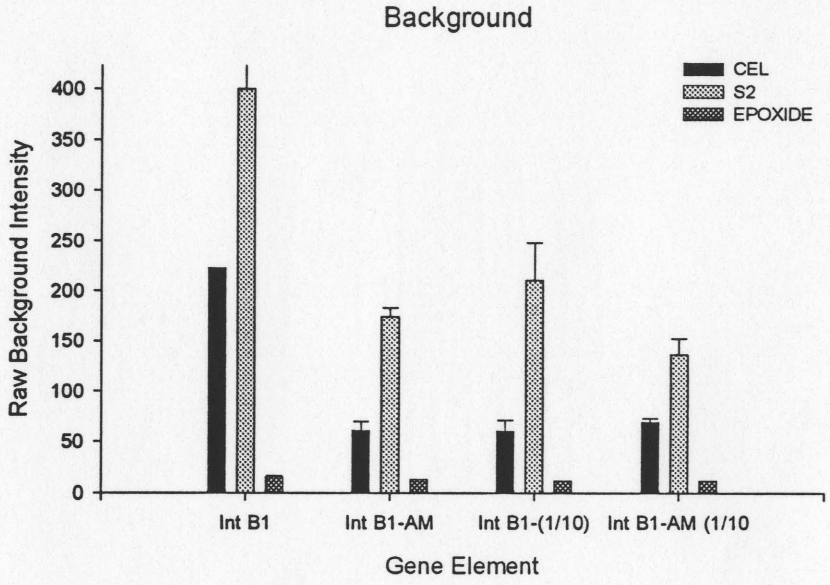

from 95-75% with a constant PMT of 85% and the slide scanned until hybridization signals dropped off in detectable value to <200 for the Integrin-β1 spots that had been diluted 100 fold and 1000 fold on the prototype microarrays. This cut-off laser intensity was determined to be 90% for epoxide I, whereby low hybridization signals could barely be detected for the 100 and 1000 fold dilution spots of Integrin-β1 (Table IV). PMT settings were determined in a similar fashion, whereby the settings were decreased incrementally from 90%-60% (with constant laser intensity of 90%) on prototype microarrays, the slides scanned, and the results obtained compared to the proper fold change patterns seen with 90-85 (laser intensity to PMT) settings. The fold change patterns were compromised when the PMT was too low or too high, as was the hybridization signal intensity when the laser intensity was too low. Thus, the settings of 90% laser intensity and 85% PMT were used since proper ratios were obtained without compromising image quality.

Verifying printing of the 58-gene Big-Array.

Labeled PCR products were hybridized to the Big-Arrays printed on epoxide I (see Materials and Methods) in equal amounts to test for cross hybridization and spot printing quality. An image of the hybridization experiment involving five elements (iNOS, Thrombospondin-1, Cadherin-VE, FLK-1, and Vez-f1) is shown in Fig. 13. Positive hybridization signal for each of the genes was present on triplicate spots, verifying that the arrayer spotted each gene correctly across three spots. No cross-hybridization was observed to other elements. The raw intensity values for the rest of the

Table IV.
Detectability of Integrin-B1 (1/100 dilution) and Integrin-B1 (1/1000 dilution) on epoxide I.

Laser Intensity	Detectable Integrin-β1 1/100 Dilution (Hybridization Signal > 200)	Detectable Integrin-β1 1/1000 Dilution (Hybridization Signal >200
95%	yes	yes
90%	yes	yes
85%	yes	no
80%	no	no
75%	no	no

Figure 13.
Hybridization of fluorescently labeled PCR products iNOS (1), Thrombospondin-1 (2), and Cadherin-VE (3) with Cy-5 (red) and FLK-1 (4) and Vez-f1 (5) with Cy-3 (green) to Big-Array 16.

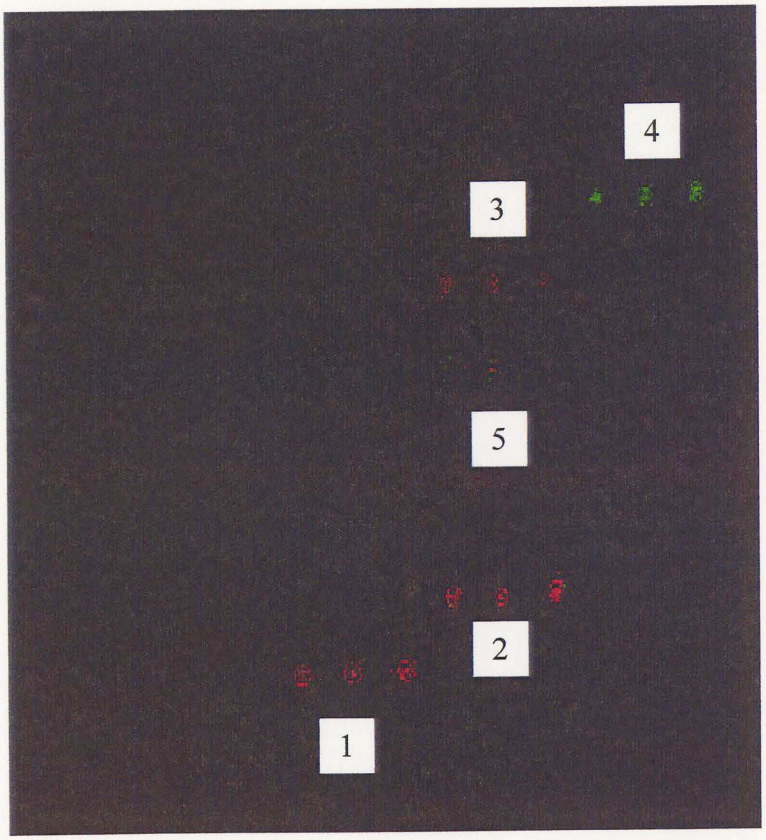

genes not hybridized to the Big-Array were equal to background levels for both the Cy-3 and Cy-5 channels. To test the precision of the Big-array, 15 μg of mouse total heart RNA was labeled in the presence of Cy-3 dCTP fluorochrome and 7.5 μg of it was hybridized to Big-Array 12 (Fig. 14). All of the genes had raw hybridization signals associated with them in varying amounts. The signals ranged from ~2000 to ~17,000 in intensity. Additionally, each of the three spots within a triplicate associated with one gene had similar hybridization signal values. Figure 15 shows the individual hybridization values of the triplicates for 5 hybridized genes. Figure 16 shows the mean of the hybridization intensities for each of the triplicate sets along with the standard deviations. No hybridization occurred to the two plant genes Thioredoxin and Chlorophyll a/b binding protein. The raw intensity values of these two genes were consistent with the low overall background signal inherent to the epoxide I slides.

To test the accuracy of the Big-Array, equal amounts (7.5 μg) of total mouse heart RNA were labeled with Cy-3 and Cy-5 and hybridized to Big-Array 23. Upon imaging the scanned slide and normalizing the data, all of the elements exhibited a yellow color, indicating equal amounts of mRNA from each sample (heart RNA, Cy-3; heart RNA, Cy-5) were hybridized to each arrayed element (Fig. 17). Raw hybridization intensities across triplicates within the microarray were very similar for each channel and mirror the small deviations obtained from Big-Array 12. A scatter plot graph of the two different fluorochrome intensities for all the genes was generated to show the correlation between the sets of data (Fig. 18). Finally, no hybridization signal was detected on the two plant control genes.

Figure 14.
Image of 7.5 ug total heart RNA labeled with Cy-5 hybridized to Big-Array 12.

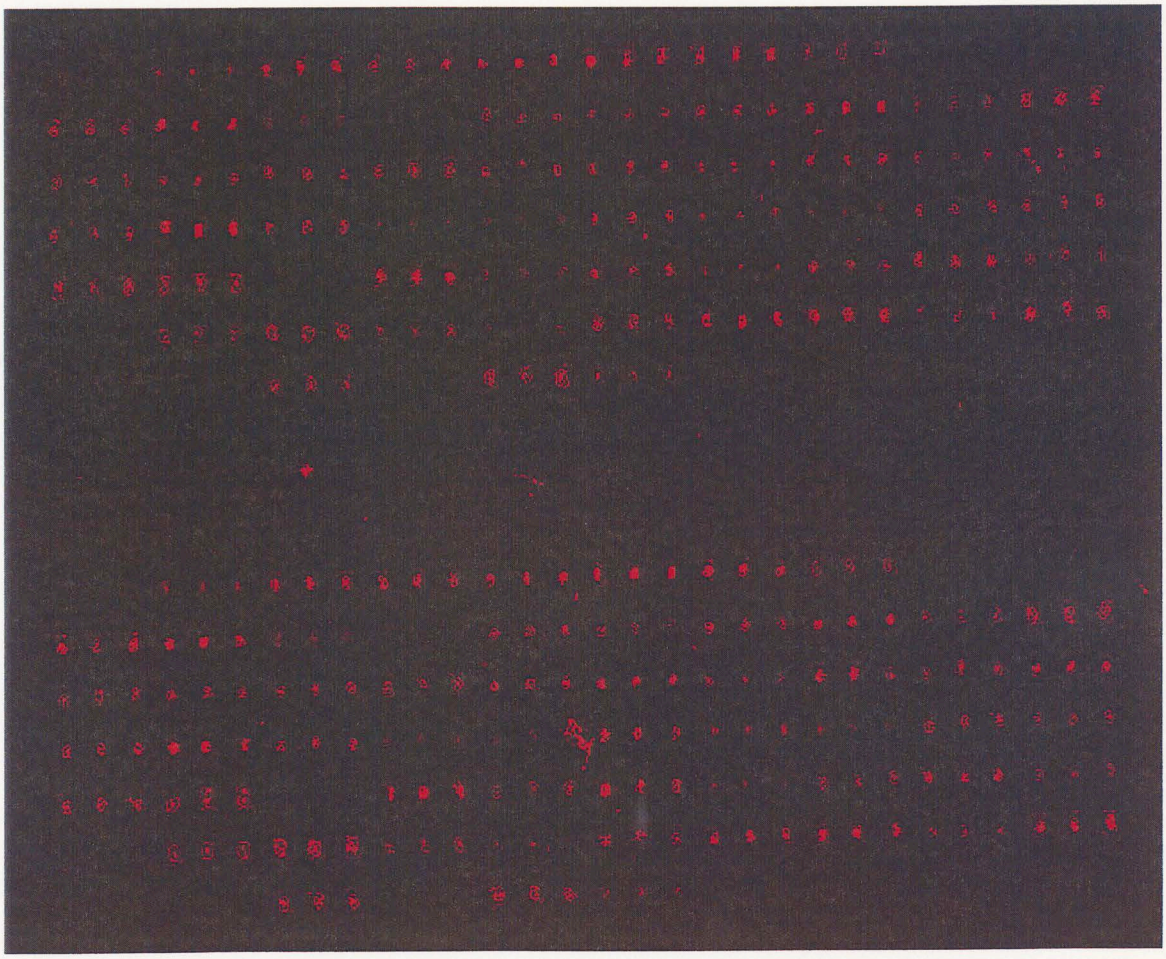

Figure 15.
Raw Cy-5 hybridization signals of 5 genes from Big-Array 12 (heart RNA) showing similar values across triplicates representing each gene.

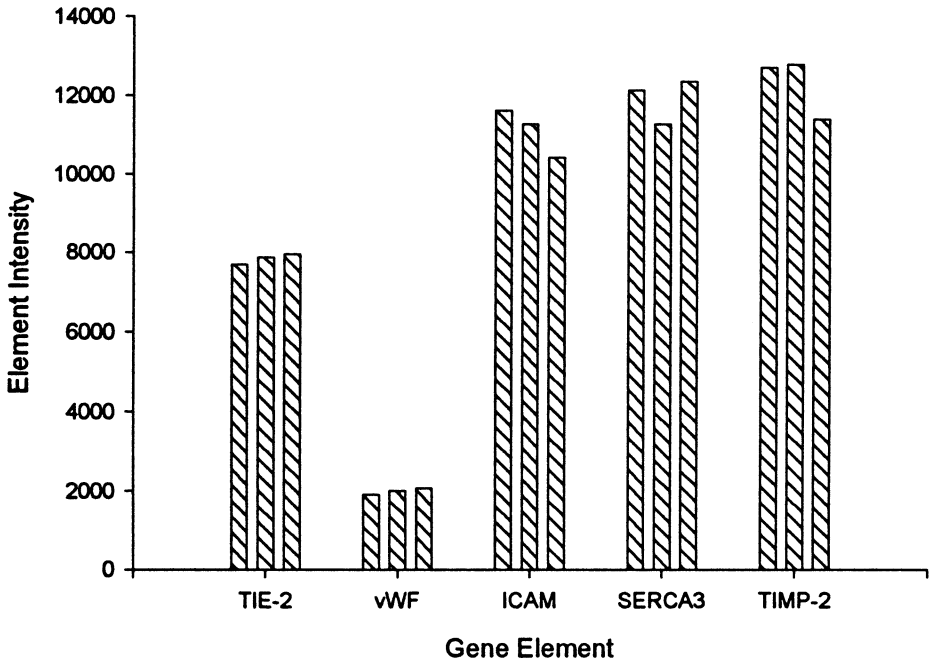

Figure 16.
Mean Cy-5 hybridization intensities with standard deviations for 5 genes on Big-Array 12.

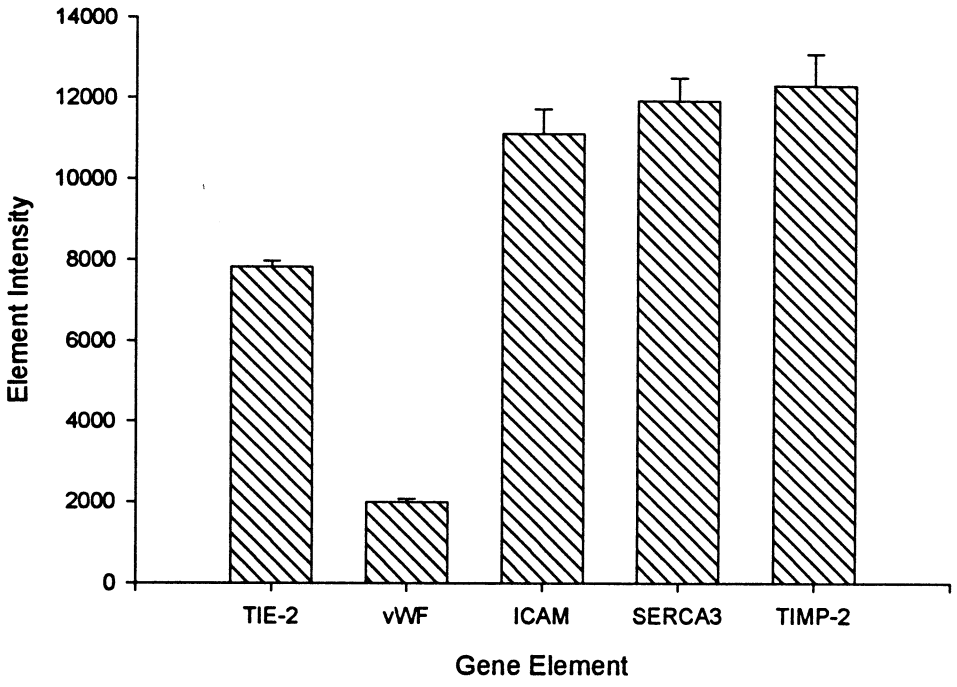

Figure 17.
Equal amounts of heart RNA labeled with Cy-3 and Cy-5 dCTP and hybridized to Big-Array 23.

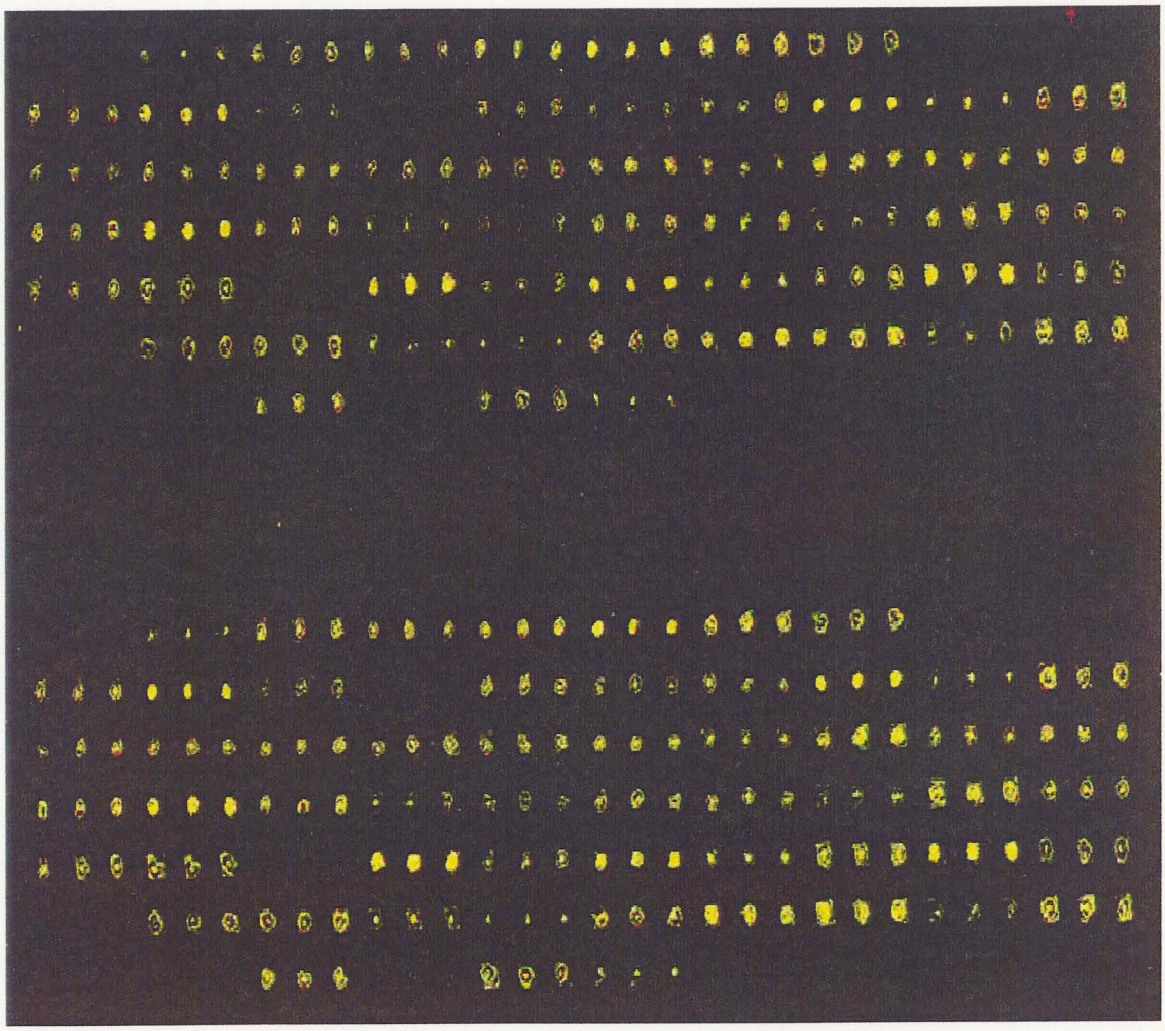

Figure 18.
Scatter plot of equal amounts of mouse heart RNA labeled with different fluorochromes and hybridized to Big-Array 23.

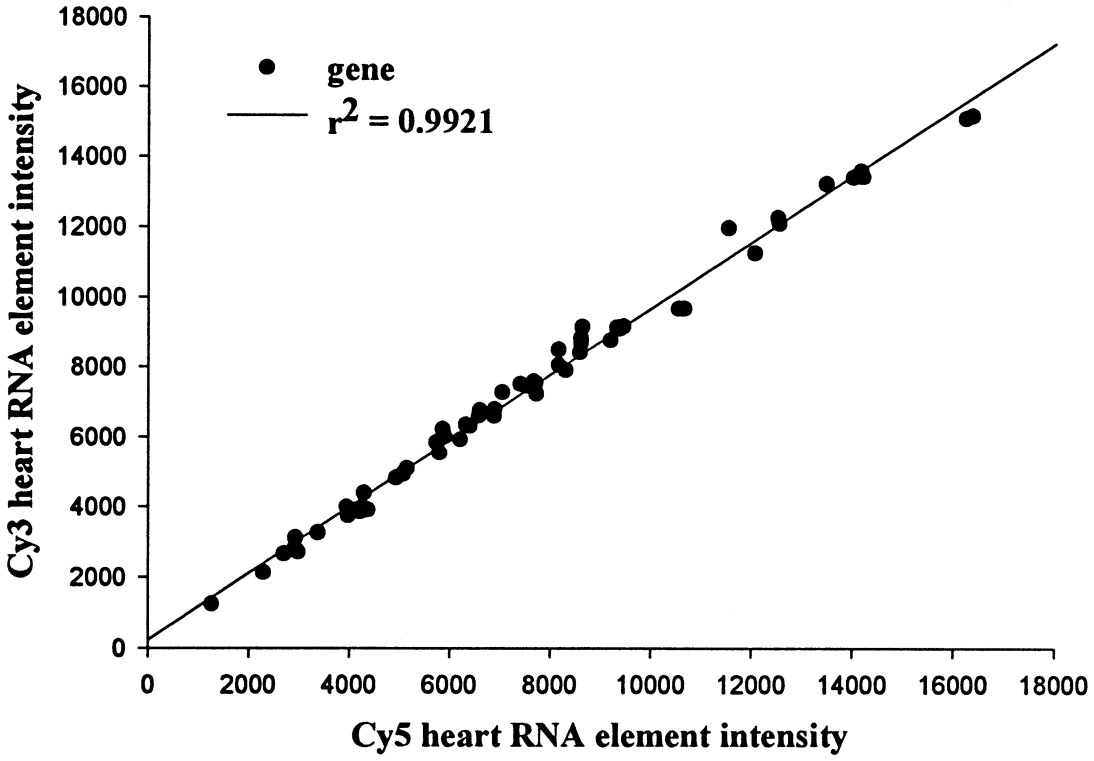

II-4 vs. Unmodified Healing Tissue.

To develop transcription profiles for the angiogenesis-related genes present on the microarray for the two different healing responses, gene expression in healing tissue surrounding II-4 modified and unmodified ePTFE polymer implants and mouse tumor versus normal muscle was compared. Unmodified ePTFE polymer implants exhibited few new blood vessels. These blood vessels were present on the luminal side of the implant only, and did not span the entire healing tissue and polymer (Fig. 19a). In contrast, II-4 modified ePTFE polymer implants exhibited numerous, large vessels in the surrounding healing tissue (Fig. 19b). This new vasculature was present mostly on the luminal side, but some vasculature existed on the abluminal side.

Differentially labeled cDNA's from II-4 and unmodified ePTFE polymer were then combined and hybridized to Big-Array 5 (Fig. 20). From the hybridization image, it can be seen that roughly half of the genes were present in equal amounts (yellow) in both samples while the other half were upregulated (green) in the II-4 modified healing tissue. After determining the exact ratios using the ScanAlyze program, 31/58 genes were upregulated at least 1.5 times (Fig. 21). For this microarray, no hybridization occurred to the negative plant control genes. Additionally, raw hybridization intensities across triplicates within each microarray were consistent as seen on the previous microarrays. Finally, the hybridization was repeated and yielded similar results.

Tumor vs. Normal Muscle.

Mouse mammary EMT6 tumor cells injected subcutaneously in the flank of a

Figure 19.
Captured images of the luminal side of the a) unmodified ePTFE and b) II-4 modified ePTFE five week polymer implants and surrounding tissue.

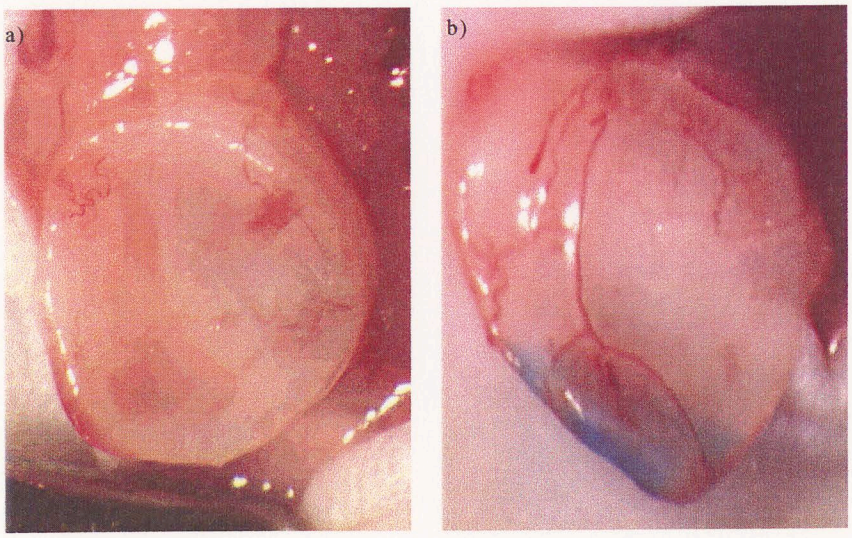

Figure 20.
Image of labeled II-4 modified ePTFE implant tissue cDNA (green) vs. labeled unmodified ePTFE implant tissue cDNA (red) hybridized to Big-Array 5.

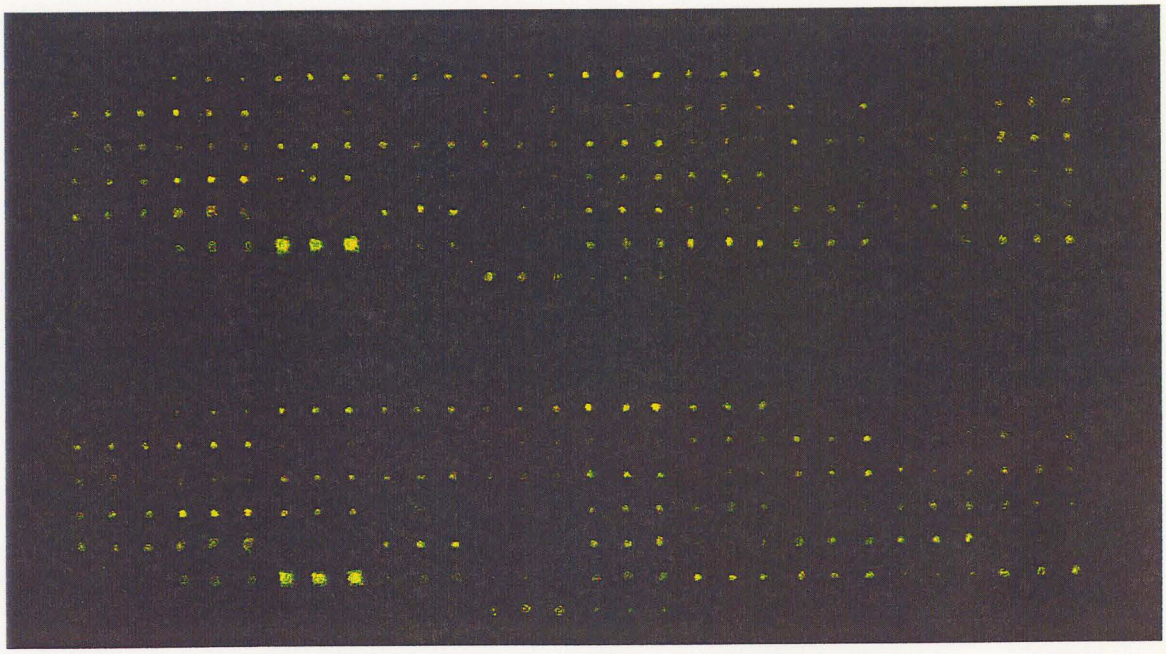

Figure 21.
Transcription profile of Unmodified vs. II-4 Modified ePTFE Implant Tissue.

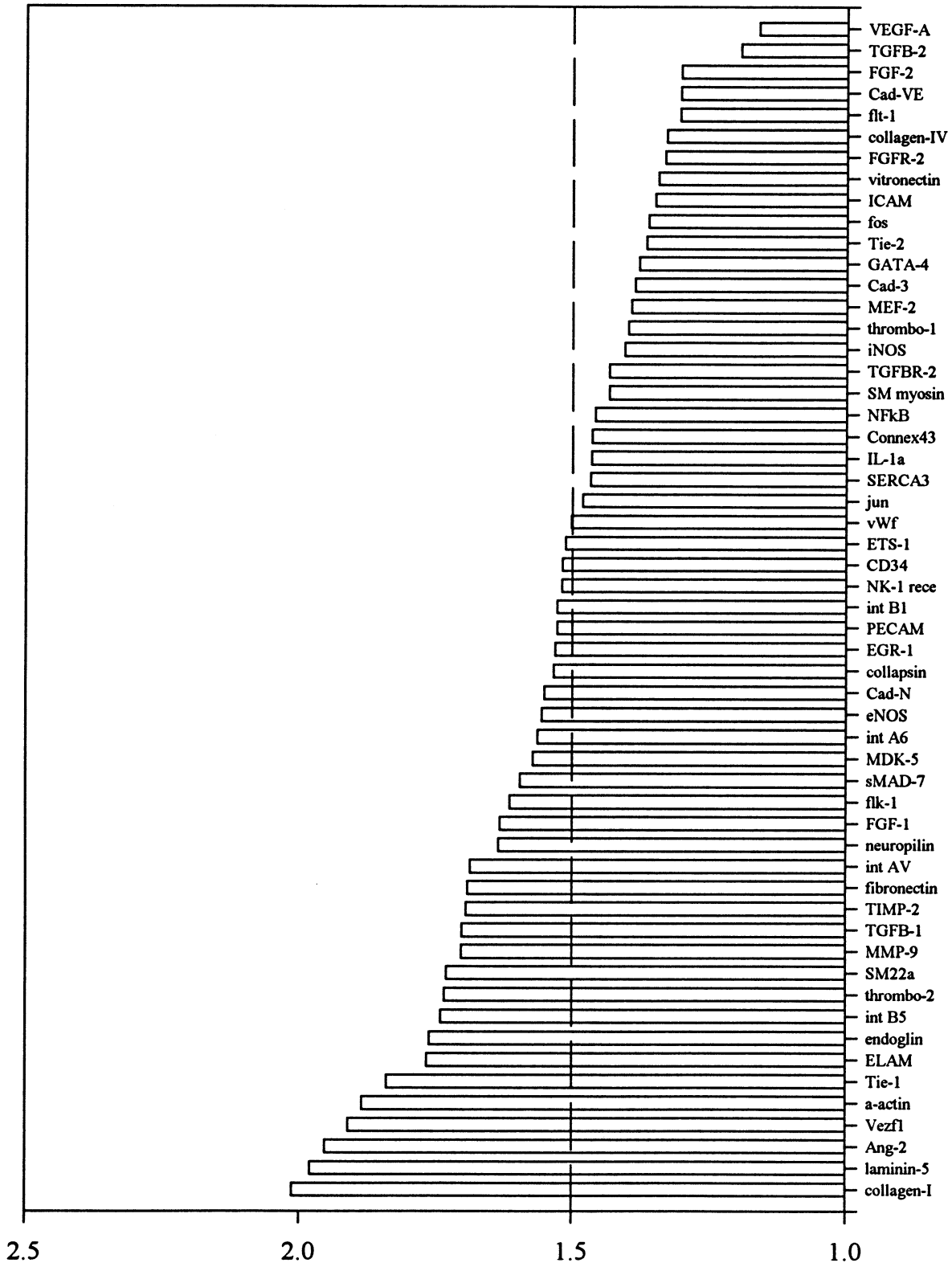

SCID mouse will grow substantially beyond 3 cm. in diameter. This growth is thought to require angiogenesis. Histology of these tumors harvested at 2-3 cm. in diameter indicated the presence numerous, small blood vessels (data not shown). To develop transcription profiles for the genes present on the microarray for the tumor and the non-angiogenic normal thigh tissue, 7.5 μg of total RNA isolated from the tumor was labeled in the presence of Cy-5 dCTP. Similarly, 7.5 μg of total RNA isolated from the normal mouse thigh tissue was labeled in the presence of Cy-3 dCTP. The labeled cDNA's were then combined and hybridized to Big-Array 42. From the image (Fig. 22) and analysis (Fig. 23), 46/58 genes are upregulated in the tumor (red), 11/58 genes are not changed from normal tissue (yellow), and 1 gene is downregulated in the tumor (green). For this microarray as seen previously, no hybridization occurred to the negative control plant genes, the overall slide background was low, and the hybridization was repeated to verify reproducibility.

Figure 22.
Image of labeled tumor tissue cDNA (red) vs. labeled mouse thigh tissue cDNA (green) hybridized to Big-Array 42.

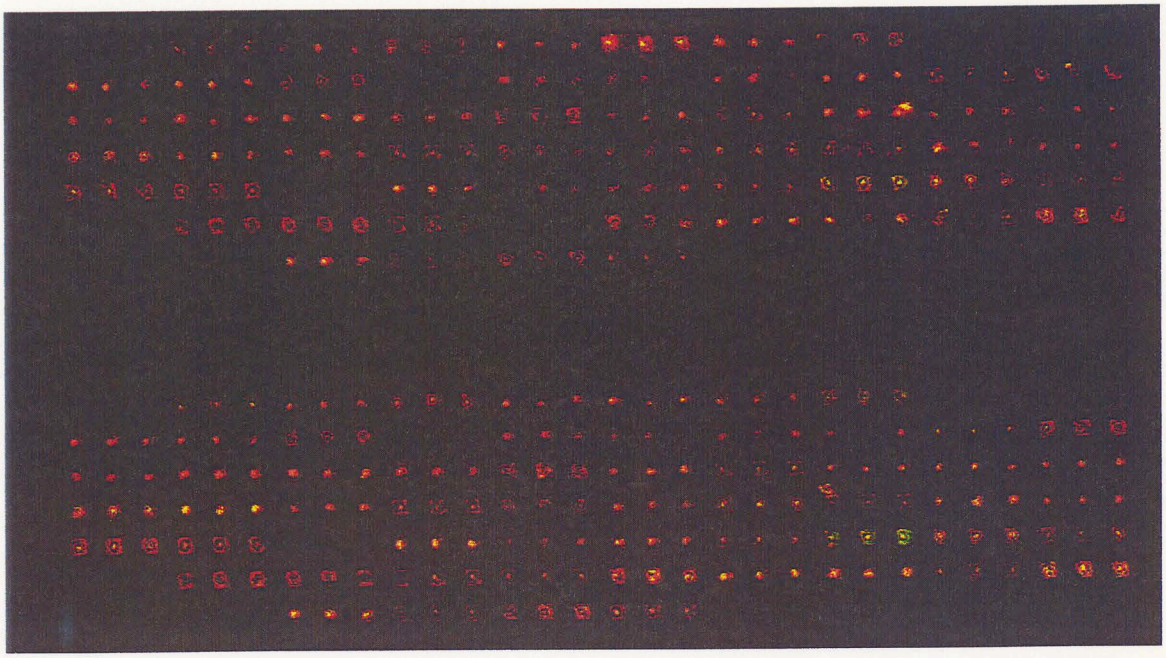

Figure 23.
Transcription Profile of Tumor vs. Mouse Thigh Tissue.

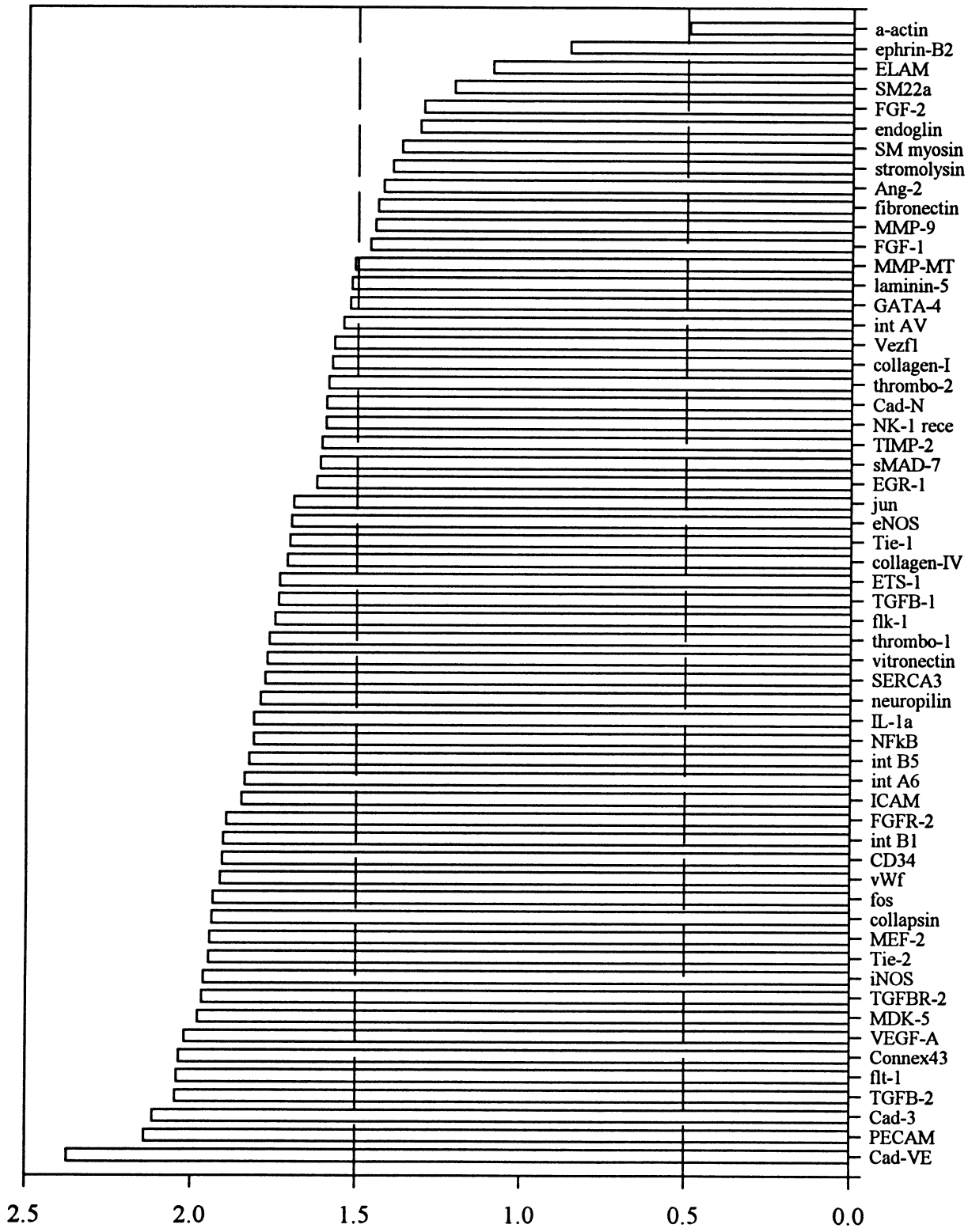

DISCUSSION

In assessing the performance of the microarrays manufactured and used in this first study, many control experiments were performed. First, prototype microarrays consisting of ten genes, two amino-modified genes, and a dilution series were printed to gain some experience with microarray technology and identify a suitable slide chemistry. These test experiments showed that no cross-hybridization was occurring on these prototypes, as the only spots to show any hybridization intensity were the spots that matched the PCR products hybridized to the microarrays. These results also gave insight as to the correct concentration with which to array the DNA elements. This concentration turned out to be 3 μg/10 μl, which is the standard within the scientific community. The dilutions allowed for the establishment of the microarray sensitivity, which was determined to be about a 1000 fold. Furthermore, the type of slide surface chemistry that yielded the optimum results was identified. The epoxide I coating, prepared in the lab, gave similar cDNA hybridization intensities and lower background intensities when compared with commercial products (S2 and CEL, Fig. 11 and 12), exhibited good precision (Figs. 15 and 16), good accuracy (Figs. 10 and 18), and did not require amino-modification of elemental DNA.

A possible explanation as to why the epoxide I coated slides performed better than the commercial slide products with respect to signal to noise ratios is due to the fact that the epoxide chosen created an extremely hydrophobic surface that covalently linked the spotted DNA immediately after printing. This hydrophobic surface allowed for

printed DNA to remain in a circular pattern consistent with the pin and not spread out over the slide after printing, causing dilution of the DNA in some areas within the spot, as can occur with charged slide surfaces such as poly-l-lysine. Thus, when hybridized, this concentrated spot of DNA was able to promote higher and more uniform intensities than a non-uniform spot. Additionally, by covalently linking the spotted DNA immediately after printing, the DNA remained firmly attached and never was able to detach. Other slide chemistries, such as CEL, which are aldehyde-based, require an additional Schiff-base reaction step to covalently link the printed DNA. This extra step may alter the fashion in which the printed DNA is attached to the slide surface in such a way as to detract from the ability of the incoming probe to hybridize, although this has been poorly characterized by the scientific community thus far. Another explanation for why the epoxide slides have a low inherent background involves the fact that the silane groups on the slide surface are extremely reactive toward the blocking agent used to inactivate the remaining reactive groups on the slide surface after printing. Once blocked, the entire slide is only reactive to incoming probe where DNA is bound, which prevents any non-specific interactions the probe can have with the rest of the slide surface. Since the epoxide was completely blocked, or at least blocked to a degree more than the commercial products, minimal noise is seen post hybridization. Finally, the epoxide I slides prepared in the lab were cost-effective. Almost all slides made were usable and cost roughly $1.10, whereas 30-40% of the CEL and poly-L-lysine slides (at a cost of $3.00 per slide when adjusted for the defective slides) commercially available and free of contaminants were usable.

A few aspects of DNA microarray technology that appear to be extremely important involve the printing tip choice and RNA quality. The printing tips used for this study were the ChipMaker 2 Microspotting pins. While these pins exhibited almost no carryover from spot to spot, the quality of the spots varied greatly. These spots ranged in size from about 50-100 microns and some were doughnut shaped. This posed problems when imaging and analyzing the hybridizations using ScanAlyze since the program requires excellent spot quality in order to extract proper data readings. For this reason alone, many hybridizations had to be repeated in order to present the program with usable hybridization spots. Currently, there are about 5 companies which manufacture microarray printing tips and for future experiments this issue needs to be resolved in order to obtain accurate data. Another issue that greatly affects hybridization results involves the RNA quality. RNA that has degraded or that is not pure can add to the overall noise of the image and cause high background signals, which will affect the accuracy of the results. Additionally, poor RNA quality may lead to an increase in cross-hybridization as this degraded RNA can take the form of an entirely different transcript and change the transcription profiles of the genes involved. Throughout the course of the study, it was learned that in order to get the best RNA for a microarray hybridization, it was necessary to extract the RNA immediately after the tissue was explanted.

Some complications associated with microarray technology, such as the incorporation rates of the two fluorochromes and the normalization of the hybridized image, remain unclear. It is still not known to what extent the incorporation rates of Cy-3 and Cy-5 dCTP's vary in the reverse transcribed cDNA and to what amount they are each

incorporated. This could potentially impact whether or not these fluorochromes are a viable way to study the changes in mRNA levels across two samples. A possible way around this problem is to use radioactivity, which is known to incorporate at a much higher amount. In this particular case, only one sample would be needed and absolute levels mRNA could be detected. The drawback to such a system is that a single sample cannot be reliably analyzed on printed DNA microarrays (such as those used in these studies) because not every spot printed on the microarrays has the same amount of DNA. Another poorly characterized issue of DNA microarrays, and a consequence of variable dye incorporation involves the normalization of the two fluorescent channels. Normalization is needed because equal amounts of Cy-3 dCTP and Cy-5 dCTP fluoresce at different amounts depending on scanner and the incorporation rates between the two flourochromes are different. The most common way to normalize a microarray hybridization is to use control housekeeping genes that do not change in concentration across the two experimental samples. Then, the entire data set is corrected to produce a ratio of 1 for these genes. However, it can be difficult to identify a gene that truly does not change in expression across different samples, making this normalization procedure difficult to use. Another way to normalize the two channels is to add up the entire amount of fluorescence present in each channel and then normalize each element value to this sum total value. Normalized values are then used to determine change in expression between the two samples (41). This method attempts to account for unknown variations in procedures and does not make any assumptions as to gene expression levels. However, because it is assumed that most genes represented on the microarray do not

change in expression, this method is best suited for large microarrays. The normalization procedure used for this study involved computing an average intensity of each channel on some of the genes that exhibited no change in expression between the samples hybridized and correcting the data to produce a ratio of 1 for these genes.

A final aspect of DNA microarray technology characterized for this study involves the amount of total RNA needed for labeling in order for the microarray to detect real changes. In this study, 15 μg of total RNA was labeled into cDNA for each fluorochrome, with 7.5 μg of each reaction (or ½ of each labeled cDNA reaction) being hybridized to each array. This amount is far below what is commonly reported by other investigators, which averages about 30-50 μg. Although 7.5 μg of total RNA is low in amount compared to others, detectable changes were seen by the microarrays used in this study. For instance, when equal amounts of two samples were labeled with different fluorochromes and hybridized, no change in the amount transcript within each sample was seen (Fig. 17). However, when the tumor tissue vs. normal thigh tissue and the II-4 modified ePTFE implant tissue vs. unmodified ePTFE tissue transcription profiles are compared, definite changes are present. This indicates that the microarray is detecting specific changes. Although there is no way to check that the microarray results are completely accurate without performing specific Northern Blots or other assays on each of the 58 genes used in this study. Reproducibility was obtained across the microarrays as well by hybridizing the remaining ½ of the labeled cDNA mixture to other microarray slides and comparing them to the original hybridizations. This ensured that the labeled cDNA came from the original reactions (since reverse transciptase reactions can vary

greatly from reaction to reaction). Also, since the chemistry used to coat the epoxide slides in the lab for this study has never been used by anyone else, it is possible that the sensitivity of these slides is better than the commercial products available.

An overall assessment of DNA microarray technology in the current scientific literature confirms that the process is still new and many improvements need to be made. Issues such as the ones encountered for this study are common to all users of this technology. Additional problems, such as the cost of supplies (which can total upwards of $120,000 for an arrayer and scanner), along with the cost of new printing tips and the fluorochromes are still very high. Furthermore, the large amounts of data that are extracted from every microarray experiment need to be analyzed and warehoused in some organized fashion. All of this, coupled with the fact that a two-dimensional, glass based slide system such as the type used for this study, may not in fact be the right approach. Currently, three dimensional polymer scaffold systems are under development, which allow for larger amounts of hybridization and higher signal intensities. This type of technology would only require the use of a configured CCD camera and not an expensive laser scanner. Technology such as this will be available in the near future. For the experiments performed here, however, the current DNA microarray technology produced useful and insightful findings worthy of future studies.

For this study, DNA microarrays were used to monitor the changes in gene expression that occur in tissue undergoing angiogenesis in order to gain insight into the complex molecular mechanisms that govern the process. By using a healing tissue response model in mice to polymer implantation as well as a controlled tumor growth

model, two different angiogenic situations were created whereby the gene expression changes between the two situations could be observed. It is clear from the results that two, completely different genetic programs were utilized by the underlying tissue cells to induce the formation of new blood vessels within each angiogenic situation. In all, 31/58 genes (53%) were upregulated at least ½ fold in the polymer implant tissue. In the tumor vs. normal thigh, 46/58 genes (79%) were upregulated at least 1/2 fold while 1 gene was downregulated at least 1 fold in the tumor tissue. When the two transcription profiles were compared against each other (Fig. 24), different genes were upregulated in the II-4 modified ePTFE vs. unmodified ePTFE healing tissue than in the tumor vs. normal thigh tissue. To further characterize the difference in two transcription profiles, a scatter plot graph was generated that shows a low correlation number of 0.34 (Fig. 25).

For these graphs, the value of 1.5X (or 0.5 fold increase) was chosen as the threshold value for detection of significant changes in gene expression levels. This value was chosen because it is conservative with respect to the actual detection limits obtained from microarrays. For the microarrays used in this study, the detection limit was probably lower. In analyzing the data associated with the mouse total heart RNA labeled with both fluorochomes and hybridized to Big-Array 23 (Fig. 17), the range of change in expression values between the two samples was only 0.3 or about 0.15 in either direction around the no change in expression axis. Therefore, it is possible that other genes are changing significantly in expression levels between the two angiogenesis environments studied, but the threshold value of 1.5 is eliminating them.

Figure 24.
Gene expression differences between the two angiogenesis phenotypes observed in this study.

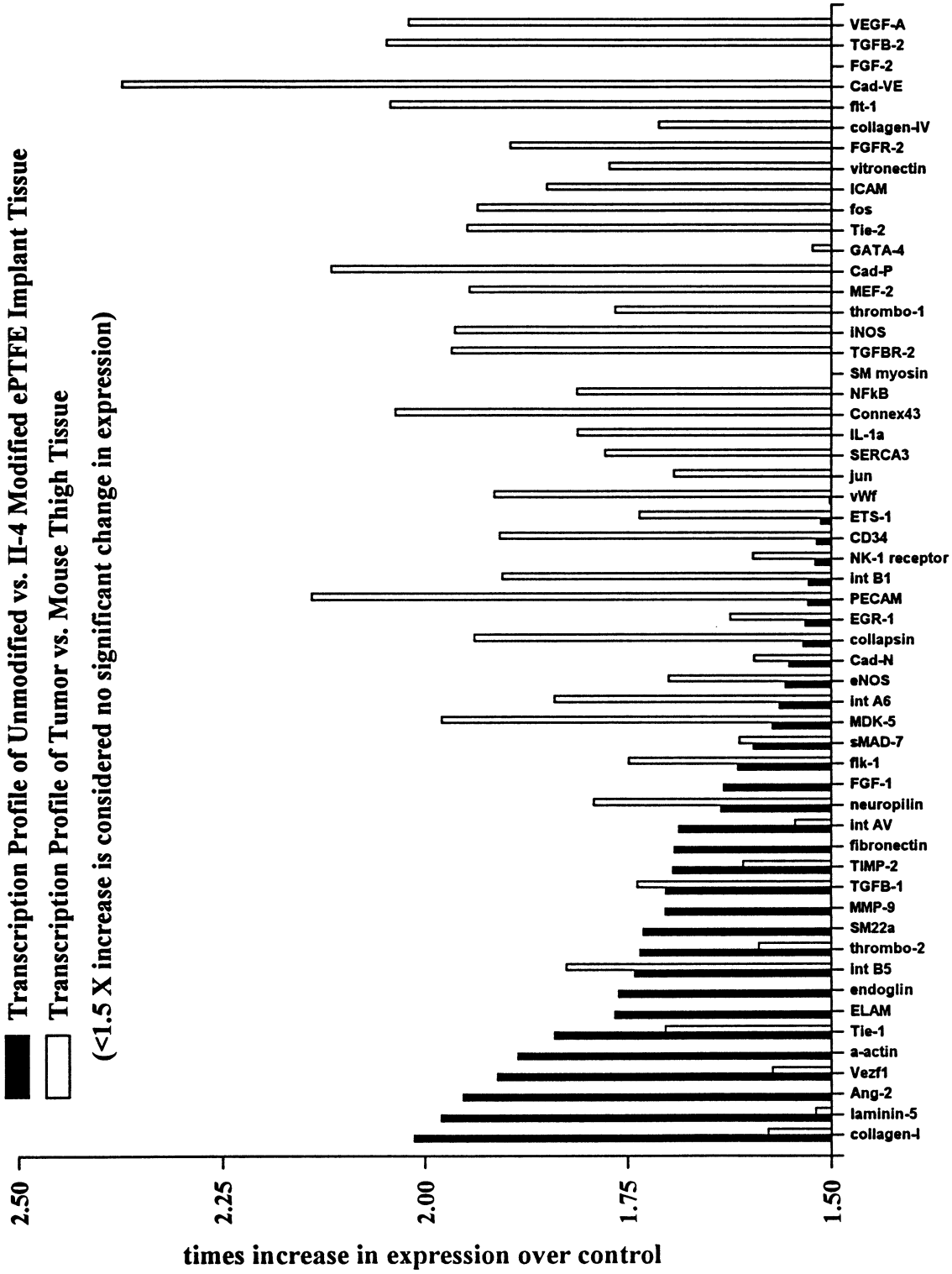

Figure 25.
Scatter plot of Figure 24 data showing a low correlation between the two types of angiogenesis environments studied.

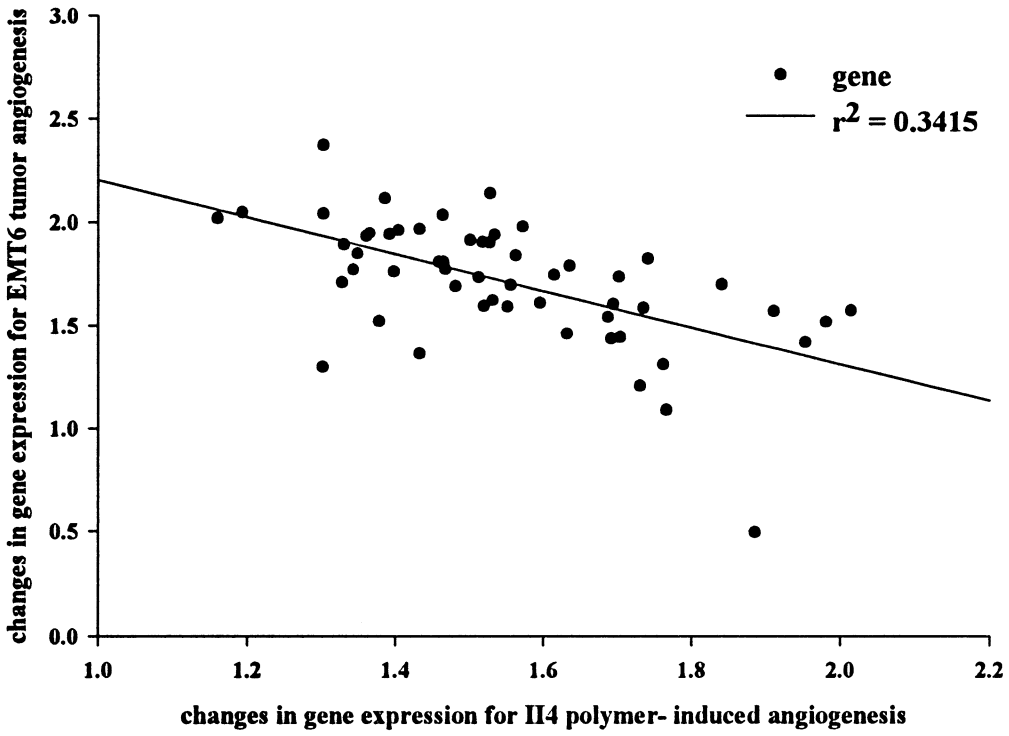

Certain patterns of genes were also revealed between the two angiogenic environments. For example, smooth muscle cell specific marker gene transcripts for SM22α and α-actin were both upregulated in the polymer implant healing tissue at five weeks while SMC-myosin exhibited slightly under no change. In the tumor tissue, SM22α and SMC-myosin exhibited no change while a-actin was downregulated. These preliminary results suggest that the polymer implant tissue formed a more mature vasculature. Further analysis revealed that the transcripts for cadherin-VE and cadherin-3 exhibited no change in the polymer implant tissue while cadherin-N was upregulated slightly. In the tumor tissue, however, Cadherin-VE and Cadherin-3 were upregulated over 1 fold, while Cadherin-N was upregulated slightly. This large difference in the presence of Cadherins, which are cell-cell adhesion molecules, may further suggest that the stability (and in fact the maturity) of the vasculature in the polymer implant tissue at five weeks is greater than that of the tumor vasculature. Genes that were upregulated significantly in both cases were Integrin B5, TIE-1, TGFB-1, TIMP-2, FLK-1, and Neuropilin. Although it is difficult to pinpoint whether these are a coordinated group of genes required for all types of angiogenesis to occur from this study, these results suggest that these six genes may be important in the angiogenic process.

Clearly, expression of mRNA alone is not sufficient to establish functional associations among proteins, since the amount of mRNA transcribed does not always correlate to the amount of protein translated (44). Additionally, this survey only constituted 58 genes thought relevant to angiogenesis by an intense literature search and probably represents less than 1% of the entire mouse genome. Finally, no effort was

made to select specific cDNA's made by healing tissue or tumor tissue, so certain specific genes relevant to these situations may have been missed. In lieu of this, however, the type of expression data presented here is very useful as a preliminary study and does provide the basis for further hypotheses. Furthermore, the interplay of particular groups of genes in the angiogenic process can be elicited from this small group of genes, as evidenced by the differential expression of transcription factors in both situations, such as ETS-1, which is required for the formation of new blood vessels (30). Coordinated changes in expression of many genes may be due to the action of a single or small amount of transcription factors (such as ETS-1) and this type of interplay could be elicited from the microarray used in this study with the help of a SOM or some type of cluster analysis software. In order to obtain information on all of the genes involved for the two types of angiogenesis situations looked at for this study, and thus a more complete study of angiogenesis, the entire mouse genome would need to be printed on DNA microarrays. This would involve making a normalized cDNA library and establishing a way to retrieve, store, and analyze the data. These types of experiment would yield a wealth of information about the physiology and pathology of angiogenesis. Additionally, the establishment of other models for studying angiogenesis, such as ischemic tissue and natural wound healing responses, combined with DNA microarrays, would further contribute to a greater understanding of the complex process of angiogenesis.

APPENDIX A
Primer Sequences

Gene Name	Forward Primer	Reverse Primer
Angiopoetin-2	agcagctgagagctcaggac	tttgtgctgctgtctggttc
Endoglin	aggtgacgtttaccaccagc	gtggttgccattcaagtgtg
Integrin A6	accgaggtcacctttgacac	ggcacctgatgttcacacac
Integrin AV	acactttgggctgtggaatc	cgccacttaagaagcacctc
Integrin B1	tgggacaggagaaaatggac	gcattcacaaacacgacacc
Integrin B5	agtactttggcaatccacgg	gcttcctcacttcctcgttg
Laminin-5	accacctctgaacaccaagg	attggctaggaccacgtgac
Tie-1	aacggttctcaccaggtcac	tgacagctctgtccaaaacg
Tie-2	gagacagaccctgcttttgc	cttctccctccagcactgtc
Cadherin-N	agggtggacgtcattgtagc	atttgcagtgttcctgtccc
Cadherin-VE	cttcaagctgccagaaaacc	aaactgcccatacttgaccg
Cadherin-3	gatgatggggaccatttcac	tgatgttcagcacttgaggc
CD34	ctgacttgagaaagctgggg	atgccactttcctgcatacc
Vitronectin	tgtttgagcactttgccttg	tgggtagggaggattcacag
Fibronectin	accagattggtgactcctgg	tgtggttcatctccctcctc
Connexin-43	tggacaaggtccaagcctac	gacgtgagaggaagcagtcc
ETS-1	agtggacagaaacccacgtc	tgcaaggtgtctgtctggag
FGF-1	ctgaagagtgggcgtaggag	tggatactcaggaaaacccg
FGF-2	agcggctctactgcaagaac	tatggccttctgtccaggtc

Gene Name	Forward Primer	Reverse Primer
FGFR-2	tgtctgcaaggtttacagcg	gaagtctggcttcttggtcg
FLK-1	tctttcggtgtgttgctctg	tctgtctggctgtcatctgg
FLT-1	acgatggcaacagggtagac	atctatggtcttcccccacc
PECAM	ctgagcctagtgtggaagcc	gccattaactagcgcctctg
SM22	ggctcaattcttgaaggcag	ggctaaggataggtgggagc
sMAD-7	tcctgctgtgcaaagtgttc	ttgttgtccgaattgagctg
TGFβ-1	tgagtggctgtcttttgacg	tggttgtagagggcaaggac
TGFβ-2	acttttgaccgtgaagtggc	gacgcagaaaaggctgaaac
TGFβR-2	atgcatccatccacctaagc	atgacagctatggcaatccc
VEGF-A	agcacagcagatgtgaatgc	aggaatcccagaaacaaccc
EGR-1	tggtggagacgagttatccc	aggtctccctgttgttgtgg
ELAM-1	tggtagttgcactttctgcg	gagagcacctccaccttctg
ICAM	cctgtttcctgcctctgaag	gtctgctgagacccctcttg
NFkB	ccttctaaaggctggtgctg	aatagacccaccaagtcccc
Vezf1	tgcatgagtgaggagaccag	atgtcataggagtgggcagg
Ephrin-B2	acaggtgggaggtgactgac	tgctttgctttgacatggag
iNOS	gtggtgacaagcacatttgg	ggctggacttttcactctgc
eNOS	tctgtcagttcagcacccag	ctgtcctcaggaggtcttgc
SMC-myosin	caagaagcaggaactggagg	cagctgcatcttgagctctg
Thrombospondin-1	tcaagtttgcaacaagcagg	tgtcatagtcttcctgcccc
Thrombospondin-2	gaaccagctgagcaagaacc	atgaagaccagggtgaccag

Gene Name	Forward Primer	Reverse Primer
TIMP-2	gcatcacccagaagaagagc	tgtccctccagacccactac
Collagen-I	actggtacatcagcccgaac	atatttttggcttttggggg
Collagen-IV	aggatgcaacggtacaaagg	tttttcaccgtctttcccag
IL-1α	tctttgaagttgacggaccc	aggccacaggtattttgtcg
MEF-2	ggaagcggaatgagagacag	tcgggaaaactggaacagac
Collapsin-1	cagccatgtacaacccagtg	ggctctctgtgacttcggac
MMP-9	caatccttgcaatgtggatg	attttggaaactcacacgcc
MMP-MT	agtcagggtcacccacaaag	catcactgcccatgaatgac
fos	aaaacaaacaaacccgcaag	tcatttcctcgttgggtctc
jun	tcccctatcgacatggagtc	aaagtccatcgttctggtcg
GATA-4	tctcactatgggcacagcag	cttttccagagctccacctg
MDK-5	acgctgaaggtgggatacac	tcatatcccagtagggtcgc
Neuropilin	ggagctactgggctgtgaag	agagccggacatgtgatacc
NK-1 Receptor	cgtggttgtgtgtaccttcg	tgaccttgtacacgctgctc
Stromelysin	caggtgtggtgttcctgatg	gccttggctgagtggtagag
SMC α-Actin	agacagctatgtgggggatg	gaaggaatagccacgctcag
vWF	aacggaagtccatggttctg	agtgtttgtcctattgccgc
SERCA	gccaccctggctgaacccttggctgc	ttcccctcctggactcagcttctggg
Cy-3 Oligo	cgggatggatcttgaagggg	
Cy-5 Oligo	cttcgattatcttcaagagg	

APPENDIX B
Protocols

1) cDNA synthesis for PCR

1 µl	embryo RNA (~1 µg)
1 µl	oligo-dT (~0.5 µg) (Gibco BRL)
8 µl	nuclease free H_20

Heat for 10 minutes at 65° C. Then quick chill on ice and add the following:

4 µl	5X 1st strand reaction buffer (Gibco BRL)
2 µl	100 mM DTT
0.8 µl	25 mM dNTP mix
0.5 µl	RNase Inhibitor (40 U/µl, Promega)
0.5 µl	Superscript II RT (200 U/µl, Gibco BRL)

Incubate at 42° C for 1 hour and then at 95° C for 5 minutes.

2) 100 µl PCR reactions

10 µl	10X PCR buffer
10 µl	2.5 mM dNTP's
10 µl	10 µM forward primer
10 µl	10 µM reverse primer
54 µl	dH_20
1 µl	Taq Polyemrase (.4U/rxn, 5U/µl)
5 µl	cDNA
100 µl Total	

3) Labeling of PCR products with a Fluorochrome

2 µl	10X PCR buffer
2.5 µl	2.0 mM low C dNTP's*
2 µl	10 µM Forward Primer
2 µl	10 µM Reverse Primer
10.3 µl	dH_20

0.2 µl	Taq Polymerase (.4U/rxn, 5U/µl)
1 µl	cDNA
0.5 µl	Cy-3 or Cy-5 (1 mM)
20.5 µl Total	

*low C dNTP mix:

20 µl of 100 mM A,T, G nucleotides (Amersham)
10 µl of 100 mM C nucleotide (Amersham)
930 µl dH_20

4) Labeling of Total RNA with Fluorochrome

To a PCR tube, add:

15 µg Total RNA
up to 11 µl DEPC-treated H_20
2.5 µl Oligo-dT (500 µg/mL) (Gibco BRL)

Heat mixture for 10 minutes at 70° C. Transfer to ice for 30 seconds.

Add the following:

3.0 µl	Cy-3 or Cy-5 (1 mM)
6.0 µl	5X 1st Stand Buffer (Gibco BRL)
3.0 µl	DTT (100 mM)
0.6 µl	25 mM low C dNTP's*
2.0 µl	Superscript II RT (200 U/µl, Gibco BRL)
1 µl	RNase Inhibitor (40 U/µl, Promega)
Total: ~30 µl per tube	

Incubate at 42° C for 2 hours. Place on ice.

REFERENCES

1. Ahlswede, K.M. and S.K. Williams. 1994. Microvascular endothelial cell sodding of 1-mm expanded polytetrafluoroethylene vascular grafts. *Arterioscler.Thromb.* 14:25-31.

2. Asahara, T., D. Chen, T. Takahashi, K. Fujikawa, M. Kearney, M. Magner, G.D. Yancopoulos, and J.M. Isner. 1998. Tie2 receptor ligands, angiopoietin-1 and angiopoietin-2, modulate VEGF- induced postnatal neovascularization [see comments]. *Circ Res* 83:233-240.

3. Bartosiewicz, M., M. Trounstine, D. Barker, R. Johnston, and A. Buckpitt. Development of a Toxicological Gene Array and Quantitative Assessment of This Technology. *Arch.Biochem.Biophys.2000.Apr.1.;376.(1.):66.-73.* 376:66-73.

4. Bassett, D.E.J., M.B. Eisen, and M.S. Boguski. 1999. Gene expression informatics--it's all in your mine. *Nat.Genet.* 21:51-55.

5. Boswell, C.A. and S.K. Williams. 1999. Denucleation promotes neovascularization of ePTFE in vivo. *J Biomater.Sci.Polym.Ed.* 10:319-329.

6. Carmeliet, P. and D. Collen. 1997. Molecular analysis of blood vessel formation and disease. *Am.J Physiol.* 273:H2091-H2104

7. Chee, M., R. Yang, E. Hubbell, A. Berno, X.C. Huang, D. Stern, J. Winkler, D.J. Lockhart, M.S. Morris, and S.P. Fodor. 1996. Accessing genetic information with high-density DNA arrays. *Science* 274:610-614.

8. Claverie, J.M. 1999. Computational methods for the identification of differential and coordinated gene expression [In Process Citation]. *Hum.Mol.Genet.* 8:1821-1832.

9. DeRisi, J., L. Penland, P.O. Brown, M.L. Bittner, P.S. Meltzer, M. Ray, Y. Chen, Y.A. Su, and J.M. Trent. 1996. Use of a cDNA microarray to analyse gene expression patterns in human cancer [see comments]. *Nat.Genet.* 14:457-460.

10. DeRisi, J.L., V.R. Iyer, and P.O. Brown. 1997. Exploring the metabolic and genetic control of gene expression on a genomic scale. *Science* 278:680-686.

11. Duggan, D.J., M. Bittner, Y. Chen, P. Meltzer, and J.M. Trent. 1999. Expression profiling using cDNA microarrays. *Nat.Genet.* 21:10-14.

12. Eisen, M.B. and P.O. Brown. 1999. DNA arrays for analysis of gene expression. *Methods Enzymol.* 303:179-205:179-205.

13. Ermolaeva, O., M. Rastogi, K.D. Pruitt, G.D. Schuler, M.L. Bittner, Y. Chen, R. Simon, P. Meltzer, J.M. Trent, and M.S. Boguski. 1998. Data management and analysis for gene expression arrays. *Nat.Genet.* 20:19-23.

14. Folkman, J. 1982. Angiogenesis: initiation and control. *Ann.N.Y.Acad.Sci.* 401:212-27:212-227.

15. Folkman, J. 1985. Tumor angiogenesis. *Adv.Cancer Res* 43:175-203:175-203.

16. Folkman, J. and R. Cotran. 1976. Relation of vascular proliferation to tumor growth. *Int.Rev.Exp.Pathol.* 16:207-48:207-248.

17. Folkman, J. and P.A. D'Amore. 1996. Blood vessel formation: what is its molecular basis? [comment]. *Cell* 87:1153-1155.

18. Folkman, J. and C. Haudenschild. 1980. Angiogenesis in vitro. *Nature* 288:551-556.

19. Folkman, J. and M. Klagsbrun. 1987. Angiogenic factors. *Science* 235:442-447.

20. Folkman, J. and Y. Shing. 1992. Angiogenesis. *J Biol Chem* 267:10931-10934.

21. Gimbrone, M.A.J., R.S. Cotran, S.B. Leapman, and J. Folkman. 1974. Tumor growth and neovascularization: an experimental model using the rabbit cornea. *J Natl.Cancer Inst.* 52:413-427.

22. Greenblatt, M. and P. Shubi. 1968. Tumor angiogenesis: transfilter diffusion studies in the hamster by the transparent chamber technique. *J Natl.Cancer Inst.* 41:111-124.

23. Hanahan, D. 1997. Signaling vascular morphogenesis and maintenance [comment]. *Science* 277:48-50.

24. Hanahan, D. and J. Folkman. 1996. Patterns and emerging mechanisms of the angiogenic switch during tumorigenesis. *Cell* 86:353-364.

25. Heller, R.A., M. Schena, A. Chai, D. Shalon, T. Bedilion, J. Gilmore, D.E. Woolley, and R.W. Davis. 1997. Discovery and analysis of inflammatory disease-related genes using cDNA microarrays. *Proc.Natl.Acad.Sci.U.S.A.* 94:2150-2155.

26. Herblin, W.F. and J.L. Gross. 1994. Inhibition of angiogenesis as a strategy for tumor growth control. *Mol.Chem Neuropathol.* 21:329-336.

27. Lockhart, D.J., H. Dong, M.C. Byrne, M.T. Follettie, M.V. Gallo, M.S. Chee, M. Mittmann, C. Wang, M. Kobayashi, H. Horton, and E.L. Brown. 1996. Expression monitoring by hybridization to high-density oligonucleotide arrays [see comments]. *Nat.Biotechnol.* 14:1675-1680.

28. Loftus, S.K., Y. Chen, G. Gooden, J.F. Ryan, G. Birznieks, M. Hilliard, A.D. Baxevanis, M. Bittner, P. Meltzer, J. Trent, and W. Pavan. 1999. Informatic selection of a neural crest-melanocyte cDNA set for microarray analysis. *Proc.Natl.Acad.Sci.U.S.A.* 96:9277-9280.

29. Luo, L., R.C. Salunga, H. Guo, A. Bittner, K.C. Joy, J.E. Galindo, H. Xiao, K.E. Rogers, J.S. Wan, M.R. Jackson, and M.G. Erlander. 1999. Gene expression profiles of laser-captured adjacent neuronal subtypes [published erratum appears in Nat Med 1999 Mar;5(3):355]. *Nat.Med.* 5:117-122.

30. Oda, N., M. Abe, and Y. Sato. 1999. ETS-1 converts endothelial cells to the angiogenic phenotype by inducing the expression of matrix metalloproteinases and integrin beta3. *J Cell Physiol.* 178:121-132.

31. Ono, M., H. Torisu, J. Fukushi, A. Nishie, and M. Kuwano. 1999. Biological implications of macrophage infiltration in human tumor angiogenesis. *Cancer Chemother.Pharmacol.* 43 Suppl:S69-71:S69-S71

32. Pepper, M.S. 1997. Manipulating angiogenesis. From basic science to the bedside. *Arterioscler.Thromb.Vasc.Biol* 17:605-619.

33. Perou, C.M., S.S. Jeffrey, M. van de Rijn, C.A. Rees, M.B. Eisen, D.T. Ross, A. Pergamenschikov, C.F. Williams, S.X. Zhu, J.C. Lee, D. Lashkari, D. Shalon, P.O. Brown, and D. Botstein. 1999. Distinctive gene expression patterns in human mammary epithelial cells and breast cancers. *Proc.Natl.Acad.Sci.U.S.A.* 96:9212-9217.

34. Ribatti, D., A. Vacca, L. Roncali, and F. Dammacco. 1991. Angiogenesis under normal and pathological conditions [published erratum appears in Haematologica 1991 Sep-Oct;76(5):following 445]. *Haematologica* 76:311-320.

35. Risau, W. 1997. Mechanisms of angiogenesis. *Nature* 386:671-674.

36. Salzmann, D.L., L.B. Kleinert, S.S. Berman, and S.K. Williams. 1997. The effects of porosity on endothelialization of ePTFE implanted in subcutaneous and adipose tissue. *J Biomed.Mater.Res* 34:463-476.

37. Salzmann, D.L., D.C. Yee, D.J. Roach, S.S. Berman, and S.K. Williams. 1998. Healing response associated with balloon-dilated ePTFE. *J Biomed.Mater.Res* 41:364-370.

38. Sato, T.N., Y. Tozawa, U. Deutsch, K. Wolburg-Buchholz, Y. Fujiwara, M. Gendron-Maguire, T. Gridley, H. Wolburg, W. Risau, and Y. Qin. 1995. Distinct roles of the receptor tyrosine kinases Tie-1 and Tie-2 in blood vessel formation. *Nature* 376:70-74.

39. Schena, M., D. Shalon, R.W. Davis, and P.O. Brown. 1995. Quantitative monitoring of gene expression patterns with a complementary DNA microarray [see comments]. *Science* 270:467-470.

40. Schena, M., D. Shalon, R. Heller, A. Chai, P.O. Brown, and R.W. Davis. 1996. Parallel human genome analysis: microarray-based expression monitoring of 1000 genes. *Proc.Natl.Acad.Sci.U.S.A.* 93:10614-10619.

41. Sehl, P.D., J.T. Tai, K.J. Hillan, L.A. Brown, A. Goddard, R. Yang, H. Jin, and D.G. Lowe. Application of cDNA microarrays in determining molecular phenotype in cardiac growth, development, and response to injury [In Process Citation]. *Circulation 2000.Apr.25.;101.(16.):1990.-9.* 101:1990-1999.

42. Shalaby, F., J. Rossant, T.P. Yamaguchi, M. Gertsenstein, X.F. Wu, M.L. Breitman, and A.C. Schuh. 1995. Failure of blood-island formation and vasculogenesis in Flk-1-deficient mice. *Nature* 376:62-66.

43. Southern, E., K. Mir, and M. Shchepinov. 1999. Molecular interactions on microarrays. *Nat.Genet.* 21:5-9.

44. Stanton, L.W., L.J. Garrard, D. Damm, B.L. Garrick, A. Lam, A.M. Kapoun, Q. Zheng, A.A. Protter, G.F. Schreiner, and R.T. White. Altered Patterns of Gene Expression in Response to Myocardial Infarction. *Circ Res 2000.May.12.;86.(9.):939.-945.* 86:939-945.

45. Wang, H.U., Z.F. Chen, and D.J. Anderson. 1998. Molecular distinction and angiogenic interaction between embryonic arteries and veins revealed by ephrin-B2 and its receptor Eph-B4 [see comments]. *Cell* 93:741-753.

46. Wang, J.L., Y.H. Liu, M.C. Lee, T.M. Nguyen, C. Lee, A. Kim, and M. Nguyen. Identification of Tumor Angiogenesis-Related Genes by Subtractive Hybridization. *Microvasc.Res 2000.May.;59.(3.):394.-397.* 59:394-397.

47. Weidner, N., J.P. Semple, W.R. Welch, and J. Folkman. 1991. Tumor angiogenesis and metastasis--correlation in invasive breast carcinoma. *N.Engl.J Med.* 324:1-8.

48. Welford, S.M., J. Gregg, E. Chen, D. Garrison, P.H. Sorensen, C.T. Denny, and S.F. Nelson. 1998. Detection of differentially expressed genes in primary tumor tissues using representational differences analysis coupled to microarray hybridization. *Nucleic.Acids.Res.* 26:3059-3065.

49. White, K.P., S.A. Rifkin, P. Hurban, and D.S. Hogness. 1999. Microarray analysis of Drosophila development during metamorphosis. *Science* 286:2179-2184.

50. Whitney, L.W., K.G. Becker, N.J. Tresser, C.I. Caballero-Ramos, P.J. Munson, V.V. Prabhu, J.M. Trent, H.F. McFarland, and W.E. Biddison. 1999. Analysis of gene expression in mutiple sclerosis lesions using cDNA microarrays. *Ann.Neurol.* 46:425-428.

51. Yancopoulos, G.D., M. Klagsbrun, and J. Folkman. 1998. Vasculogenesis, angiogenesis, and growth factors: ephrins enter the fray at the border [comment]. *Cell* 93:661-664.

52. Zetter, B.R. 1988. Angiogenesis. State of the art. *Chest* 93:159S-166S.